bioRxiv preprint doi: https://doi.org/10.1101/2022.03.09.483541; this version posted October 3, 2024. The copyright holder for this preprint (which was not certified by peer review) is the author/funder, who has granted bioRxiv a license to display the preprint in perpetuity. It is made available under aCC-BY-NC-ND 4.0 International license.

Odors drive feeding through gustatory receptor neurons in *Drosophila*

Hong-ping Wei[1], Thomas Ka Chung Lam[2], and Hokto Kazama[1,3,4,*]

[1]RIKEN Center for Brain Science, 2-1 Hirosawa, Wako, Saitama, 351-0198, Japan.

[2]Neuroengineering Laboratory, Brain Mind Institute & Interfaculty Institute of Bioengineering, EPFL, Lausanne, Switzerland

[3]RIKEN CBS-KAO Collaboration Center, 2-1 Hirosawa, Wako, Saitama, 351-0198, Japan.

[4]Graduate School of Arts and Sciences, The University of Tokyo, 3-8-1 Komaba, Meguro-ku, Tokyo, 153-8902, Japan.

*Correspondence: hokto.kazama@riken.jp

Summary

Odors are intimately tied to the taste system to aid food selection and determine the sensory experience of food. However, how smell and taste are integrated in the nervous system to drive feeding remains elusive. We show in *Drosophila* that odors alone activate gustatory receptor neurons (GRNs), trigger proboscis extension reflex (PER), a canonical taste-evoked feeding behavior, and enhance food intake. Odor-evoked PER requires the function of sugar-sensing GRNs but not olfactory organs. Calcium imaging and electrophysiological recording show that GRNs directly respond to odors. Odor-evoked PER is mediated by the Gr5a receptor, and is bidirectionally modulated by olfactory binding proteins. Finally, odors and sucrose co-applied to GRNs synergistically enhance PER and food consumption. These results reveal a cell-intrinsic mechanism for odor-taste multimodal integration that takes place as early as in GRNs, indicating that unified chemosensory experience is a product of layered integration in peripheral neurons and in the brain.

bioRxiv preprint doi: https://doi.org/10.1101/2022.03.09.483541; this version posted October 3, 2024. The copyright holder for this preprint (which was not certified by peer review) is the author/funder, who has granted bioRxiv a license to display the preprint in perpetuity. It is made available under aCC-BY-NC-ND 4.0 International license.

Introduction

Feeding behavior is an outcome of intricate interactions among multiple external and internal senses (Boesveldt and de Graaf, 2017; McCrickerd and Forde, 2016; Spence, 2015). Of particular relevance is an interplay between the senses of smell and taste. Olfactory and gustatory systems prime feeding by signaling food presence, guiding food choice, and inducing anticipatory responses in digestive organs (Boesveldt and de Graaf, 2017; McCrickerd and Forde, 2016). During consumption, they synergistically define the sensory experience of food together with other cues (Spence, 2015). Although imaging studies have identified neural correlates of odor-taste interaction in the brain (Small, 2012), mechanistic understanding of chemosensory integration is still lacking.

Drosophila offers an attractive model to address this issue, where peripheral chemosensory systems are well-characterized (Scott, 2018; Wilson, 2013), and feeding behavior can be quantified by measuring the strength of proboscis extension reflex (PER) (Dethier, 1976) and the amount of subsequent food consumption. PER is an initial step of feeding evoked by the presentation of sugar to the proboscis or legs housing gustatory receptor neurons (GRNs). Previous studies reported that odors increase the rate of PER (Oh et al., 2021; Reisenman and Scott, 2019; Shiraiwa, 2008) as well as food intake (Reisenman and Scott, 2019), exemplifying olfactory enhancement of feeding in *Drosophila*. However, aside from the involvement of olfactory receptor neurons (Oh et al., 2021; Shiraiwa, 2008), biological mechanisms underlying this multisensory enhancement remain elusive.

Here we investigated the impact of odors on feeding behavior and found direct contribution of GRNs to odor-evoked PER, odor-taste integration, and odor-driven enhancement of food consumption, indicating that multisensory integration commences at the very periphery.

Results

Odors alone evoke PER

To examine how odors affect PER, we built a behavioral recording setup in which a tastant and multiple odors with diverse innate values (Badel et al., 2016) can be applied to individual, tethered flies (Figure 1A). To quantify the movement of proboscis, we used a deep learning-based, markerless pose estimation algorithm (Mathis et al., 2018) and tracked the trajectory of three segments constituting the proboscis. The angles made between the segments (rostrum, haustellum, and labellum angles) were subsequently calculated over time to detect PER (Figures

bioRxiv preprint doi: https://doi.org/10.1101/2022.03.09.483541; this version posted October 3, 2024. The copyright holder for this preprint (which was not certified by peer review) is the author/funder, who has granted bioRxiv a license to display the preprint in perpetuity. It is made available under aCC-BY-NC-ND 4.0 International license.

1A-1C; see Methods for the definition of PER). Unexpectedly, we found that the odors alone evoked repetitive PER without an application of a tastant (Figures 1D-1G, and Movie S1). Different odors evoked PER with different probability (Figure 1E), latency (Figure S1A), and duration (Figures 1F, 1G, and S2). Stimulus-triggered PER was not observed in response to solvents or air (Figure 1D-1G). Odors evoked PER even at the concentration of 10^{-2}, which induce stimulus-specific activity in the olfactory pathway (Badel et al., 2016; Endo et al., 2020; Kato et al., 2023). The level of PER did not correlate with the innate value of odors, previously determined by quantifying the odor preference of flies in a behavioral arena (Badel et al., 2016; Pearson's $R = 0.33$, $p = 0.52$). Odor-evoked PER was observed in other genetic backgrounds and another *Drosophila* species as well albeit at a lower level with different tuning (Figure S3).

Odor-evoked PER resembled taste-evoked PER in multiple aspects. First, its trajectory was similar to that of taste-evoked PER (Figure S1B, Movie S1) and was consistent with the reported movement of proboscis during sucrose-evoked PER (Schwarz et al., 2017). The trajectories were indistinguishable between the tested odors (Figure S1B). Second, it showed concentration dependency (Dethier, 1976; Wang et al., 2004). The probability and duration of PER increased as a function of stimulus concentration (Figures 1E and 1G). Third, it depended on the metabolic state just as taste-evoked PER (Inagaki et al., 2014). The duration of PER was higher in starved as compared to fed flies (Figure S4).

In sum, odors initiate feeding behavior in *Drosophila*.

Odors evoke PER through GRNs

To confirm that this behavior is mediated by the olfactory system, we repeated the experiment after removing the sensory organs housing the olfactory receptor neurons, namely the antennae and the maxillary palps. However, this manipulation only attenuated and did not eliminate odor-evoked PER (Figure 2A). Suppressing the activity of most olfactory receptor neurons by expressing a potassium channel Kir2.1 (Paradis et al., 2001) with *Orco-Gal4* driver (Larsson et al., 2004) gave similar results (Figures 2B and 2C). These data show that the olfactory system modulates but is not required for odor-evoked PER.

We thus turned to another chemosensory system, the gustatory system. To examine its involvement in odor-evoked PER, we expressed Kir2.1 in different types of GRNs using type-specific Gal4 drivers, each of which mediates a specific taste modality (Scott, 2018). Gr5a GRNs detect sugar and mediate food acceptance behaviors including PER (Dahanukar et al., 2001;

bioRxiv preprint doi: https://doi.org/10.1101/2022.03.09.483541; this version posted October 3, 2024. The copyright holder for this preprint (which was not certified by peer review) is the author/funder, who has granted bioRxiv a license to display the preprint in perpetuity. It is made available under aCC-BY-NC-ND 4.0 International license.

Wang et al., 2004). Suppression of Gr5a GRNs significantly reduced odor-evoked PER, indicating that sweet-sensing neurons detect odors and drive PER (Figures 2B and 2D). Bitter-sensing Gr66a GRNs, on the other hand, have been shown to inhibit sweet-evoked PER (Wang et al., 2004). However, expression of Kir2.1 in these neurons had little effect (Figures 2B and 2E). We hypothesized that this is due to our use of starved flies because Gr66a pathway is reported to be downregulated in a starved condition (Devineni et al., 2019; Inagaki et al., 2014). Indeed, flies of the same genotype showed increased PER to odors in a fed state (Figure 2H), indicating that Gr66a GRNs counteract PER. Two other tastes, water and low salt can also induce PER (Cameron et al., 2010; Wang et al., 2004), which are detected by Ppk28 and Ir94e GRNs, respectively (Cameron et al., 2010; Jaeger et al., 2018). However, suppression of these cell types did not affect odor-evoked PER (Figures 2B, 2F and 2G). Together, Gr5a GRNs enhance whereas Gr66a GRNs inhibit odor-evoked PER.

As GRNs are housed in multiple external organs including the labella at the tip of proboscis, the legs, the wing margins, and the ovipositor (Scott, 2018), we next sought to narrow down the GRNs responsible for odor-evoked PER. We found that removal of the legs and wings did not abolish the behavior (Figure S5). Moreover, activation of the ovipositor induces egg laying rather than PER (Dethier, 1976). These results suggest that GRNs act predominantly in the labella to induce odor-evoked PER.

Gustatory receptors and olfactory binding proteins mediate odor-evoked PER

We have shown that Gr5a GRNs tuned to tastes trigger PER in response to a wide range of odors. Because GRNs do not express olfactory receptors (Davie et al., 2018; Li et al., 2021; Scott et al., 2001), either gustatory receptors or some other molecules are likely to interact with odorants (Jones et al., 2007; Kwon et al., 2007). Gr5a receptor is a primary candidate as Gr5a GRNs drive odor-evoked PER (Figures 2B and 2D). Consistent with this hypothesis, odor-evoked PER was nearly undetectable in the Gr5a mutant but spared in the control (Figure 2I). This demonstrates that Gr5a receptor is necessary for odor-evoked PER.

Odorant binding proteins (OBPs) are another set of molecules that could mediate odor detection by GRNs. They are thought to bind and help transport hydrophobic odorants to chemosensory receptors through aqueous lymph (Larter et al., 2016). OBPs are expressed in taste as well as olfactory sensilla (Galindo and Smith, 2001) and modulate sugar-evoked PER (Swarup et al., 2014), raising the possibility that those in the taste sensilla also mediate odorant detection.

bioRxiv preprint doi: https://doi.org/10.1101/2022.03.09.483541; this version posted October 3, 2024. The copyright holder for this preprint (which was not certified by peer review) is the author/funder, who has granted bioRxiv a license to display the preprint in perpetuity. It is made available under aCC-BY-NC-ND 4.0 International license.

To test this, we conducted a genetic screen by expressing individual Obp RNAi constructs with *tubulin-Gal4*. We targeted 9 Obp genes that are expressed highly in the labella (Cameron et al., 2010) but in trace amounts in the antenna (Larter et al., 2016) to examine the function of OBPs in the taste sensilla. Knockdown of *Obp18a*, *Obp57d/e*, and *Obp57e* genes decreased whereas that of *Obp49a* gene increased odor-evoked PER (Figures 2J and 2K, and Figure S6). Knockdown of *Obp19b*, *Obp56g*, *Obp56h*, *Obp57a/c*, and *Obp83c* genes did not have a significant effect on odor-evoked PER (Figure 2L, and Figure S6). The increased PER following *Obp49a* knockdown likely reflects disinhibition of sweet-sensing GRNs as Obp49a mediates the inhibitory impact of bitter chemicals on the activity of sweet-sensing GRNs (Jeong et al., 2013). These results suggest that OBPs modulate odor detection by GRNs.

GRNs directly respond to odors

To gain direct evidence that GRNs respond to odors, we performed two-photon calcium imaging and single-sensillum electrophysiological recording that have complementary properties (Figures 3 and 4). Calcium imaging of GRN axons using a cell-specific driver reports the population activity of neurons but can unambiguously ascribe the signals to genetically identified GRNs. On the other hand, while single-sensillum electrophysiology cannot uniquely ascribe the signals to genetically defined GRNs, it is sensitive and fast enough to detect individual spikes.

For imaging, we expressed a calcium indicator GCaMP6s (Chen et al., 2013) in Gr5a, Gr66a, Ppk28, or Ir94e GRNs and scanned the axons in the subesophageal zone of the brain (Figure 3A). Consistent with the contribution of Gr5a and Gr66a GRNs to odor-evoked PER, robust odor responses were observed in these neurons. They responded to all the tested odors but not to control stimuli, with distinct tuning (Figures 3B-3F and Figures S7A-S7F), in a concentration-dependent manner (Figures S7G, S7H and S8). A linear combination of Gr5a and Gr66a GRN responses well predicted the magnitude of odor-evoked PER with the former and the latter contributing to enhancement and suppression of PER, respectively (Figure 3G). Odor and sucrose responses were positively correlated in Gr5a GRNs (Figure S7I). By contrast, Ppk28 and Ir94e GRNs did not respond to any odors (Figures S7J and S7K), matching their little contribution to odor-evoked PER (Figures 2B, 2F and 2G).

These responses could reflect the activity originating in GRNs or that from a central olfactory circuit impinging on GRN's presynaptic terminals. To distinguish between the two scenarios, we physically covered the maxillary palps to block the input from the olfactory organs

bioRxiv preprint doi: https://doi.org/10.1101/2022.03.09.483541; this version posted October 3, 2024. The copyright holder for this preprint (which was not certified by peer review) is the author/funder, who has granted bioRxiv a license to display the preprint in perpetuity. It is made available under aCC-BY-NC-ND 4.0 International license.

and applied odors (antennae were already removed to gain optical access to the subesophageal zone, see Methods). This manipulation had little effect on the odor responses (Figure 3D and 3F). On the other hand, the responses were eliminated after covering the labella (Figures 3D and 3F), demonstrating that GRNs themselves sense odors.

As we observed that Gr5a receptor was necessary for odor-evoked PER, we further asked whether it is required for Gr5a GRNs to respond to odors. We found that odor responses were absent in the Gr5a mutant but spared in control flies (Figure 3H). This confirms that odor responses in Gr5a GRNs depend on Gr5a receptor.

For electrophysiology, we measured odor-evoked responses from individual taste sensilla on the proboscis using tip recording, a conventional technique where a glass electrode placed on the tip of a sensillum delivers a stimulus as well as records neural responses (Figure 4; Hodgson et al., Science, 1955). We targeted large and intermediate type (L- and I-type) taste sensilla, and recorded responses to odors and sucrose. Odors were dissolved in tricholine citrate (TCC), an electrolyte that suppresses the responses of water-sensing neuron (Wieczorek and Wolff, 1989). L-type sensilla housing a sweet-sensing GRN robustly responded to sucrose, but also to two tested odors, 4-methylcyclohexanol and banana odor, at a rate higher than the solvent (Figures 4A and 4B). I-type sensilla housing sweet- and bitter-sensing GRNs also responded to odors (Figures 4A and 4C). These sensilla exhibited spikes with different amplitudes that may originate in different GRNs. This is consistent with our calcium imaging results showing that both Gr5a and Gr66a GRNs respond to odors (Figure 3). Here we counted all the spikes and did not sort them based on their amplitude and shape, because these characteristics change depending on the spiking frequency (Fujishiro et al., 1984).

In sum, recording from specific types of GRNs using calcium imaging and specific types of taste sensilla using tip recording together demonstrate that GRNs in the labella sense odors in line with a recent study using a different electrophysiological technique (Dweck and Carlson, 2023).

Odor-taste integration in single taste sensillum

We investigated whether GRNs integrate multisensory stimuli when they are presented together. We presented sucrose, banana odor or a mixture of the two to individual taste sensilla during tip recording. We found that the responses to a mixture were stronger than those to component stimuli (Figure 5). While the strength of responses varied across sensilla, responses to banana

bioRxiv preprint doi: https://doi.org/10.1101/2022.03.09.483541; this version posted October 3, 2024. The copyright holder for this preprint (which was not certified by peer review) is the author/funder, who has granted bioRxiv a license to display the preprint in perpetuity. It is made available under aCC-BY-NC-ND 4.0 International license.

odor and sucrose recorded in the same sensillum were positively correlated (Figure S9). These results suggest that GRNs function as an odor-taste multisensory integrator.

GRNs integrate multisensory input to enhance PER and food consumption

We finally asked if GRNs can enhance PER and subsequent food consumption through multisensory integration. We decided to apply a mix of banana odor and sucrose as a mimic of multisensory food stimuli in the natural environment. We confirmed that the banana odor can evoke PER and GRN responses in a concentration-dependent manner (Figure S8). We then presented sucrose solution mixed with or without a low concentration (10^{-4}) of banana odor locally to the labella (Figure 6A). Although banana odor could not evoke PER on its own at this concentration (Figure S8A), we found that the addition of banana odor increased PER to sucrose especially at low concentrations where sucrose alone can only induce unreliable PER (Figure 6B). Importantly, this enhancement was observed even after removing the olfactory organs (Figure 6B), indicating that the superadditive integration takes place in GRNs. Similar results were obtained when sucrose was mixed with different monomolecular odorants (Figures 6C and 6D).

We further examined if the amount of food consumption is also enhanced by odor-taste integration in GRNs. Using a previously reported multisensory feeding assay (Reisenman and Scott, 2019), we quantified the amount of sucrose consumed by freely behaving flies with or without odors (Figure 6E). We found that the presence of banana odor increased the amount of sucrose consumption in intact flies (Figure 6F). Critically, this effect was observed in olfactory organs-removed flies as well (Figure 6F), indicating the contribution of the gustatory system. Similar results were observed under the presence of ethyl butyrate and 4-methylcyclohexanol, with the former odor exerting a stronger impact (Figure 6G). These results suggest that GRNs serve as an initial node for odor-taste multisensory integration that shapes feeding behavior (Figure 6H).

Discussion

In terrestrial animals, it has been considered that there is a clear division of labor between the two types of chemosensory organs in sensing stimuli with distinct physical properties; the olfactory and gustatory organs sense volatile and non-volatile chemicals, respectively. Therefore, although odorants and tastants are defined by the identity of cognate organs, they are used

bioRxiv preprint doi: https://doi.org/10.1101/2022.03.09.483541; this version posted October 3, 2024. The copyright holder for this preprint (which was not certified by peer review) is the author/funder, who has granted bioRxiv a license to display the preprint in perpetuity. It is made available under aCC-BY-NC-ND 4.0 International license.

interchangeably with volatile and non-volatile chemicals. However, we found using calcium imaging and electrophysiological recording that GRNs directly detect odorants, and this drives a classical taste-induced feeding behavior, PER, as well as increased food consumption. Previous studies have also hinted that odors alone evoke PER (Oh et al., 2021), and induce activity in GRNs (Devineni et al., 2019). Thus, volatile chemicals are within the molecular receptive range of GRNs and should also be regarded as tastants based on the conventional definition. Critically, this indicates that GRNs are engaged in non-contact chemo-sensing as well, a behavioral strategy distinct from contact-based chemo-sensing.

A study applying base recording, an electrophysiological technique to record from individual taste sensilla, had reported that I-type sensilla do not respond to odorant molecules dissolved in solution (Hiroi et al., 2008). However, a recent study using the same method found that S-, I-, and L-type sensilla respond to a variety of odors applied as vapor (Dweck and Carlson, 2023). Here we found that GRNs respond to odors applied in both ways in agreement with Dweck and Carlson (2023). Although the reason behind the discrepancy is not entirely clear, one possibility is the difference between the preparation used in different studies; whereas Hiroi et al. used a severed head preparation, we as well as Dweck and Carlson used immobilized, intact flies. Because we noticed in preliminary experiments that stimulus-evoked GRN spikes become weaker over time in a head only preparation where hemolymph circulation is lost, the physiological condition of sensilla may be one of the factors underlying the discrepancy. Another possibility is a difference in genotype or genetic background. We found that the strength of odor-evoked PER is different between genetic backgrounds with w^{1118} exhibiting weaker PER than Dickinson wild type (Figure S3), implying that odor responses of GRNs vary across genetic backgrounds.

Our results showed that odor responses of Gr5a GRNs are mediated by the Gr5a receptor. This may not be totally enigmatic as gustatory and olfactory receptor genes belong to the same ancient superfamily sharing a motif in the transmembrane region (Robertson et al., 2003; Scott et al., 2001), and some gustatory receptors expressed outside of GRNs function in odor (Jones et al., 2007; Kwon et al., 2007), temperature (Ni et al., 2013), and light detection (Montell, 2021; Xiang et al., 2010). However, Gr5a is unique in that the same receptor can detect stimuli of two different sensory modalities. Furthermore, we found that OBPs enriched in the labella modulate odor-evoked PER, suggesting that OBPs in this taste organ not only link tastants with gustatory receptors (Jeong et al., 2013; Swarup et al., 2014), but also mediate detection of odors.

bioRxiv preprint doi: https://doi.org/10.1101/2022.03.09.483541; this version posted October 3, 2024. The copyright holder for this preprint (which was not certified by peer review) is the author/funder, who has granted bioRxiv a license to display the preprint in perpetuity. It is made available under aCC-BY-NC-ND 4.0 International license.

PER was evoked by all the tested odors albeit to different extents, and this likely reflects the broad odor tuning of Gr5a GRNs that drive PER (Fig. 3). The question, then, is why might it be useful to exhibit PER to such a wide variety of odors including those that are normally aversive? A likely benefit can be discussed by considering foraging behavior under natural settings. During foraging in the air, olfactory receptor neurons that are more sensitive to odors locate a potential food source together with other sensory systems. After landing on the potential food, GRNs on the legs join to assess its edibility. In parallel, GRNs on the labella sense odors and enhance the probability of PER. Given that the olfactory system most likely has already guided the animal to palatable food, keeping the GRNs broadly tuned to odors is an efficient mechanism to enhance PER. Once PER brings the labella into contact with the food, GRNs act as a multisensory integrator to make a decision on food intake (Figure 6). Because inputs from olfactory and gustatory organs interact centrally as well (Oh et al., 2021; Shiraiwa, 2008) (Figure 2A), this indicates that unified chemosensory experience is built through layered integration in different parts of the body.

Although odor detection by GRNs through gustatory receptors has not previously been reported outside of *Drosophila melanogaster*, olfactory receptors are expressed in the proboscis in multiple insects (Haverkamp et al., 2016; Kwon et al., 2006; Xia and Zwiebel, 2006). A recent study reported that olfactory receptors are also expressed and functional in cultured human fungiform and mouse taste papilla cells (Malik et al., 2019), implying that peripheral odor-taste integration may be a process incorporated in various species. These and our results reveal that GRNs should be further studied not as gustatory neurons but more broadly as chemosensory integrators.

Acknowledgments

We thank Anupama Dahanukar, Graeme Davis, Michael Dickinson, Craig Montell, Kristin Scott, the Bloomington Stock Center, and the Vienna Drosophila Resource Center for flies; RIKEN CBS-Evident Collaboration Center for imaging equipment and software; Bor-Wei Cherng for help with coding; members of the Kazama laboratory for their support and comments on the manuscript. HP.W. was supported by Grant-in-Aid for JSPS Research Fellow (JP15F15384) and RIKEN Special Postdoctoral Fellowship. This work was supported by a grant from RIKEN, Kao Corporation, Asahi Corporation, and JSPS KAKENHI Grant (JP18H02532, JP18K19502, JP21H04789) to H.K.

bioRxiv preprint doi: https://doi.org/10.1101/2022.03.09.483541; this version posted October 3, 2024. The copyright holder for this preprint (which was not certified by peer review) is the author/funder, who has granted bioRxiv a license to display the preprint in perpetuity. It is made available under aCC-BY-NC-ND 4.0 International license.

Author contributions

HP.W. and H.K. designed the study. HP.W. performed all the experiments and analyzed data except for part of the behavioral data analysis, which was performed by T.K.C.L. HP.W. and H.K. wrote the paper with input from T.K.C.L.

Declaration of interests

Authors declare that they have no competing interests.

Methods

Resource availability

Further information and requests for resources should be directed to and will be fulfilled by Hokto Kazama (hokto.kazama@riken.jp).

Materials availability

This study did not generate new unique reagents.

Data and code availability

All data reported in this paper will be shared by the lead contact upon request.
All original code has been deposited at GitHub, (https://github.com/hpwei82/2022_hpwei) and will be publicly available as of the date of publication.
Any additional information required to analyze the data reported in this study is available from the Lead Contact upon request.

Drosophila strains

Flies were maintained on standard cornmeal agar under a 12 h light, 12 h dark cycle at 25 °C. All experiments were performed on adult females 2–6 days after eclosion. Flies were obtained as described in the key resources table.

Fly stocks used in this study are as follows: Dickinson wild type (Michael Dickinson), *w*^{1118}*; P{y[+t7.7] w[+mC]=GAL4.1Uw}attP2* (Bloomington #68384), *w*^{1118}*; P{y[+t7.7] w[+mC]=p65.AD.Uw}attP40; P{y[+t7.7] w[+mC]=GAL4.DBD.Uw}attP2* (Bloomington

bioRxiv preprint doi: https://doi.org/10.1101/2022.03.09.483541; this version posted October 3, 2024. The copyright holder for this preprint (which was not certified by peer review) is the author/funder, who has granted bioRxiv a license to display the preprint in perpetuity. It is made available under aCC-BY-NC-ND 4.0 International license.

#79603), *Drosophila simulans* (Kyoto DRRG #900001), *tubulin-GAL4* (Bloomington #5138 (Lee and Luo, 1999)), *Orco-GAL4* (Bloomington #26818 (Larsson et al., 2004)), *Gr66a-GAL4* (Bloomington #57670 (Kwon et al., 2011)), *Ir94e-GAL4* (Bloomington #60725 (Jaeger et al., 2018)), *Ppk28-GAL4* (Bloomington #93020 (Cameron *et al*., 2010)), *UAS-GCaMP6s* (Bloomington #42746, 42749 (Chen et al., 2013)), *UAS-Obp49a RNAi* (VDRC #330599 (Dietzl et al., 2007)), *UAS-Obp19b RNAi* (VDRC #1823), *UAS-Obp56g RNAi* (VDRC #23206), *UAS-Obp56h RNAi* (VDRC #102562), *UAS-Obp18a RNAi* (VDRC #101628), *UAS-Obp83c RNAi* (VDRC #106866), *UAS-Obp57d/e RNAi* (VDRC #101783), *UAS-Obp57e RNAi* (VDRC #105001), *UAS-Obp57a/c RNAi* (VDRC #107489), three OBP RNAi control lines w^{1118} (VDRC #60000, control for *UAS-Obp19b RNAi* and *UAS-Obp56g RNAi*), w^{1118}*;P{VDRCsh60200attP40* (VDRC #60200, control for *UAS-Obp49a RNAi*), *y,*w^{1118}*;P{attP,y[+],w[3']}* (VDRC #60100, control for other *UAS-Obp RNAi* lines), *Gr5a-GAL4* (Kristin Scott), Gr5a mutant (Anupama Dahanukar (Dahanukar et al., 2007), *ΔEP(x)-5*) and its control (Anupama Dahanukar (Dahanukar et al., 2007), *EP(x)496*), and *UAS-Kir2.1*^{AAE}*-GFP* (Graeme Davis (Paradis et al., 2001)). All the lines except for w^{1118}, *Drosophila simulans*, *Gr5a* mutant, its control, and the *UAS-RNAi* lines were backcrossed for 6 generations to the Dickinson wild type (Dickinson, 1999).

Detailed genotypes of flies used in each experiment are listed in Table 1.

Figure	**Short genotype**
1B-1G, 2A, 4, 5, 6, S1, S2, S4, S5, S8A	Dickinson Wild type
2B, 2H	*UAS-Kir2.1/+*
S3A	w^{1118}*; P{y[+t7.7] w[+mC]=GAL4.1Uw}attP2*
S3B	w^{1118}*; P{y[+t7.7] w[+mC]=p65.AD.Uw}attP40;* *P{y[+t7.7] w[+mC]=GAL4.DBD.Uw}attP2*
S3C	*Drosophila simulans*
2C, S4A, S4B	*Orco-Gal4/UAS-Kir2.1*
2D	*Gr5a-Gal4/UAS-Kir2.1*
2E, 2H	*Gr66a-Gal4/UAS-Kir2.1*
2F	*Ppk28-Gal4/UAS-Kir2.1*

bioRxiv preprint doi: https://doi.org/10.1101/2022.03.09.483541; this version posted October 3, 2024. The copyright holder for this preprint (which was not certified by peer review) is the author/funder, who has granted bioRxiv a license to display the preprint in perpetuity. It is made available under aCC-BY-NC-ND 4.0 International license.

2G	*Ir94e-Gal4/UAS-Kir2.1*
2I	*ΔEP(x)-5* *EP(x)496*
2J, S6C	*tubulin-Gal4/y,w^{1118};P{attP,y[+],w[3']}*
2J	*tubulin-Gal4/UAS-Obp57d/e RNAi*
2K	*tubulin-Gal4/w^{1118};P{VDRCsh60200}xattP40*
	tubulin-Gal4/UAS-Obp49a RNAi
2L, S6A	*tubulin-Gal4/w^{1118}*
2L	*tubulin-Gal4/UAS-Obp19b RNAi*
3A-3D, 3G, S7A-S7C, S7G, S7I, S8B	*Gr5a-Gal4;UAS-GCaMP6s*
3E, 3F, S7D-S7F, S7H	*UAS-GCaMP6s;Gr66a-Gal4*
3H	*ΔEP(x)-5;Gr5a-Gal4;UAS-GCaMP6s* *EP(x)496;Gr5a-Gal4;UAS-GCaMP6s*
S5B	*tubulin-Gal4/UAS-Obp56g RNAi*
S5D	*tubulin-Gal4/UAS-Obp18a RNAi*
S5E	*tubulin-Gal4/UAS-Obp56h RNAi*
S5F	*tubulin-Gal4/UAS-Obp83c RNAi*
S5G	*tubulin-Gal4/UAS-Obp57e RNAi*
S5H	*tubulin-Gal4/UAS-Obp57a/c RNAi*
S7J	*UAS-GCaMP6s;Ppk28-Gal4*
S7K	*UAS-GCaMP6s;Ir94e-Gal4*

Table 1. Genotypes used to generate data presented in each figure

Examination of odor-evoked PER

Virgin females that had been raised on food for 1-3 days were starved for 24-28 h in vials with water supplied through a wet piece of Kimwipe. Individual flies were briefly anesthetized on ice and their dorsal side of the thorax was attached to a cover glass with ultraviolet-curing adhesive (NOA 63, Norland), after which the flies were allowed to rest for an hour. Prior to recording odor-evoked PER, flies were water satiated until they did not consume any more. Subsequently, 100 mM sucrose solution, which acted as a positive control stimulus, was applied either on the fly's legs or proboscis (without letting the fly consume it) to examine if the fly could exhibit

bioRxiv preprint doi: https://doi.org/10.1101/2022.03.09.483541; this version posted October 3, 2024. The copyright holder for this preprint (which was not certified by peer review) is the author/funder, who has granted bioRxiv a license to display the preprint in perpetuity. It is made available under aCC-BY-NC-ND 4.0 International license.

tastant-evoked PER. Flies were discarded if they did not exhibit PER to this stimulus. Flies showing excessive spontaneous PER before the assay were also discarded. The tethered fly was positioned horizontally in air facing an odor delivery tube (Figure 1A) except for the experiment in Figure S2 where the fly was positioned vertically to mimic the preparation used in a previous study (Oh et al., 2019). The tip of the odor tube was placed 10 mm away from the fly. A monochrome camera (Lu070M, Lumenera corporation) taking a lateral view of the fly at 20 Hz was used to record the movement of proboscis in response to odors.

To examine the contribution of olfactory organs to odor-evoked PER (Figures 2 and 6), the third antennal segments and maxillary palps were removed with forceps while the flies were anesthetized on ice. After the surgery, the flies were given an hour to recover before the experiment.

To examine the contribution of GRNs on wings and legs to odor-evoked PER (Figure S4), wings and tarsal segments were removed with forceps while the flies were anesthetized on ice. After the surgery, the flies were given an hour to recover before the experiment.

Individual flies went through an experiment consisting of three blocks. In each block, 6 odors (see below), two solvent controls (mineral oil and water), and another control stimulus (air) were applied for 2 s per trial in a randomized order with a 15 s inter-trial-interval.

Olfactory stimulation

Odors were delivered with a custom-made, multi-channel olfactometer controlled by a PC as previously described (Badel et al., 2016). Briefly, an air stream (300 ml/min) was passed through 4 ml of odor solution diluted with mineral oil (nacalai tesque, 23334-85) or water. The concentration of odor was varied between 10^{-4}, 10^{-2}, 10^{-1}, and 0.5 (v/v), but the default was 0.5 unless otherwise noted. The odorized air was further diluted by mixing it with a main air stream (500 ml/min), a small portion of which was delivered frontally to the fly through an outlet placed 10 mm away from the fly. The speed of odorized air flow at the position of the fly was 0.6 m/s. Using the photoionization detector (200B miniPID, Aurora Scientific Inc.), the time odors reach the position of the fly was estimated to be 1.1 s after the odor valve opening. The odors used in the study and their abbreviations are as follows: 2-pentanone (2PT, Wako, 13303743), 3-octanol (OCT, Tokyo chemical industry, O0121), 4-methylcyclohexanol (MCH, Sigma-Aldrich, 153095), banana essence (Narizuka corporation), benzaldehyde (BNZ, Sigma-Aldrich, 418099), ethyl butyrate (EBR, Sigma-Aldrich, E15701), and isopentyl acetate (IPA, Wako, 016-03646), 1-

bioRxiv preprint doi: https://doi.org/10.1101/2022.03.09.483541; this version posted October 3, 2024. The copyright holder for this preprint (which was not certified by peer review) is the author/funder, who has granted bioRxiv a license to display the preprint in perpetuity. It is made available under aCC-BY-NC-ND 4.0 International license.

hexanol (Tokyo chemical industry, H0130), ethyl acetate (Tokyo chemical industry, A0030), yeast (nacalai tesque, M1E8921), fenchone (Tokyo chemical industry, F0164), isoamyl alcohol (Tokyo chemical industry, I0289), phenethyl alcohol (Tokyo chemical industry, P0084).

Examination of multisensory PER

To examine how flies respond to odor-taste multimodal stimuli presented to GRNs in the labella, individual flies were gently attached to a cover glass vertically by wrapping their thorax with a piece of parafilm, and multimodal stimuli were applied by touching the ventral part of the labellum with a wick made of Kimwipe immersed in a sucrose solution with or without odors (Figure 4A; (Shiraiwa, 2008)). A constant air stream (0.5~0.7 m/s) was applied with an air pump (eAir6000, GEX) from behind the wick. The legs of the flies were tucked under the parafilm to prevent them from touching the wick. The flies were allowed to rest for an hour after fixation. The concentration of sucrose was varied between 0.25-2% (v/v, Figure 6B) or fixed at 0.25% (Figures 6C and 6D) depending on the experiment. When the concentration of sucrose was varied, the stimuli were applied in an ascending order to avoid adaptation. The concentration of the added odor was 10^{-4} for all the tested stimuli. Each stimulus was applied 3 times with an inter-trial-interval of 15 s. PER was manually scored when the proboscis was fully extended within ~2 s from the stimulation.

Quantification of PER

A markerless pose estimation algorithm DeepLabCut v2.0 was used to quantify the movement of the proboscis. The position and orientation of three segments of the proboscis, the rostrum, the haustellum, and the labellum were characterized by tracking six points, namely the proximal end of the antenna, the distal end of the antenna, the rostrum apex, the rostrum-haustellum joint, the haustellum-labellum joint, and the distal end of the labellum (Figures 1B and 1C). These six points were manually labeled on the lateral view of the fly to generate the training dataset, which consisted of 1465 labeled frames in video data from 19 flies. The ResNet50 based pose estimation neural network was trained for about 200,000 iterations, after which the six points were automatically tracked in all the frames in video data.

Following the pose estimation, data were analyzed using custom code written in Python. To detect proboscis extensions, the rostrum angle (the angle made by the line passing through the proximal and distal ends of the antenna and the line along the rostrum), the haustellum angle (the

bioRxiv preprint doi: https://doi.org/10.1101/2022.03.09.483541; this version posted October 3, 2024. The copyright holder for this preprint (which was not certified by peer review) is the author/funder, who has granted bioRxiv a license to display the preprint in perpetuity. It is made available under aCC-BY-NC-ND 4.0 International license.

angle between the rostrum and the haustellum), and the labellum angle (the angle between the haustellum and the labellum) were calculated over time (see Figure 1B). The baseline of each proboscis angle was calculated as the 25th percentile of a rolling 5 s time window. The proboscis extension was defined as PER if the haustellum angle exceeded 100° because it corresponded to full extension by visual inspection. PER duration was defined as the time during which the fly exhibited PER in each second. Integrated PER duration was defined as the sum of PER duration over 4 s starting 1 s after the odor onset. These values were averaged across three trials for each odor in each fly. PER probability was defined as the percentage of trials in which PER was observed for each stimulus in each fly.

Because repetitive, spontaneous PER occurring at regular intervals represented an abnormal condition, flies showing such repetitive, spontaneous PER in more than 9 trials were excluded from further analysis.

To examine if the movement of the proboscis is similar between odor-evoked and tastant-evoked PER as well as between PER evoked by different odors, temporal sequences of the rostrum and the haustellum angles during PER and partial proboscis extensions were clustered with K-medoids clustering (Park and Jun, 2009). PER and partial proboscis extensions were detected from the baseline subtracted rostrum angle using hysteresis thresholding with a lower threshold of 5° and an upper threshold of 15°. Because the length of a temporal sequence is different between PER, the data were converted to a distance metric using dynamic time warping (Mearns et al., 2020; Sakoe and Chiba, 1978) with a warping window of 0.25 s prior to clustering. The optimal number of clusters was determined using the elbow method.

Immunohistochemistry

To examine the expression pattern of Gal4 driver lines, we performed immunohistochemistry as described previously (Badel et al., 2016) using rat anti-GFP (1:1,000, nacalai tesque, 04404-84) and mouse nc82 (1:20, Developmental Studies Hybridoma Bank at Univ. of Iowa) as primary antibodies, and anti-rat CF488A (1:250, Biotium, 20023) and anti-mouse CF633 (1:250, Biotium, 20120) as secondary antibodies. Brains were dissected out from the head capsule in phosphate-buffered saline (PBS, nacalai tesque, 2757531), fixed with 4% paraformaldehyde in PBS (nacalai tesque, 915414) for 90 min on ice, and incubated in blocking solution containing 5% normal goat serum (Invitrogen, 50197Z) in PBST (0.2% Triton X-100 (nacalai tesque,

bioRxiv preprint doi: https://doi.org/10.1101/2022.03.09.483541; this version posted October 3, 2024. The copyright holder for this preprint (which was not certified by peer review) is the author/funder, who has granted bioRxiv a license to display the preprint in perpetuity. It is made available under aCC-BY-NC-ND 4.0 International license.

3550102) in PBS) for 30 min. Primary antibodies were then added and incubated at 4 ^{o}C for ~48 h. After removing antibodies and washing over an hour, the brains were incubated in a solution of secondary antibodies at 4 ^{o}C for 24 h. The brains were immersed in Vectashield (Vector laboratories, H-1000), sealed with a cover glass, and imaged with a confocal microscope (FV3000, Olympus). Images were analyzed with Fiji (Schindelin et al., 2012).

Fly preparation for calcium imaging

Individual flies starved for 24-28 h with water were anesthetized on ice, and their dorsal side of the thorax was fixed to a piece of parafilm with ultraviolet-curing adhesive (NOA 63, Norland). The legs of the fly were covered with another piece of parafilm. The fly was subsequently attached to a custom-made recording plate in a vertical position such that the anterior part of the head was accessible through a small hole on the recording plate (Figure 3A). The proboscis was pulled out gently with forceps and immobilized in an extended position using a strip of parafilm with the labella exposed to the air. After covering the head with saline containing 103 mM NaCl, 3 mM KCl, 5 mM N-tris (hydroxymethyl) methyl-2-aminoethane-sulfonic acid, 8 mM trehalose, 10 mM glucose, 26 mM $NaHCO_3$, 1 mM NaH_2PO_4, 1.5 mM $CaCl_2$, and 4 mM $MgCl_2$ (osmolarity adjusted to 270-275 mOsm), the antennae and the associated cuticle were removed to expose the subesophageal zone. Saline was bubbled with 95% O_2/5% CO_2 and perfused at a rate of 2 ml/min during the recording.

Two-photon calcium imaging

Calcium imaging of GRN axons in the subesophageal zone was conducted using a two-photon microscope (LSM 7 MP, Zeiss) equipped with a piezo motor (P-725.2CD PIFOC, PI) that drives a water immersion objective lens (W Plan-Apochromat, 20x, numerical aperture 1.0) along the z-axis. The fluorophore was excited with a titanium:sapphire pulsed laser (Chameleon Vision II, Coherent) mode-locked at 930 nm. The laser power measured at the back aperture of the objective lens was below 20 mW. Fluorescence was collected with a GaAsP detector through a bandpass emission filter (BP470-550). Five optical slices separated by 5 μm were scanned every 500 ms. The odor delivery system was identical to that used in behavioral experiments. Sucrose was presented by a syringe whose movement was controlled by an actuator.

Image processing

bioRxiv preprint doi: https://doi.org/10.1101/2022.03.09.483541; this version posted October 3, 2024. The copyright holder for this preprint (which was not certified by peer review) is the author/funder, who has granted bioRxiv a license to display the preprint in perpetuity. It is made available under aCC-BY-NC-ND 4.0 International license.

Calcium imaging data were analyzed using custom code written in MATLAB (MathWorks). Images were registered within and across trials to correct for movement in the x-y plane as well as in depth by determining the shift along three dimensions that maximizes the correlation between the images. The region of interest (ROI) was set to cover the GRN axons in the subesophageal zone. The size of ROI was 80 × 60 μm for Gr5a GRNs, 60 × 40 μm for Gr66a GRNs, 80 × 60 μm for Ir94e GRNs, and 80 × 40 μm for Ppk28 GRNs, respectively. The average pixel intensity within the ROI was calculated for each time frame. The average of 5 frames preceding a stimulus was used as the baseline signal to calculate ΔF/F for each time frame. The peak stimulus response was quantified by averaging ΔF/F across five frames at the peak, followed by averaging across three trials for each stimulus.

Food consumption assay

Food consumption was quantified in principle as described in a previous study (Reisenman and Scott, 2019). Briefly, virgin females that had been raised on food for 1-2 days were starved for 24-28 h in vials with water supplied through a wet piece of Kimwipe. Flies were then transferred to a custom-made vial (n = 10 to 15 per vial) with a filter paper (3 cm in diameter) on the top and a small mesh tube attached laterally near the top (Figure 6E). The filter paper on the top was impregnated with sucrose solution (0.1%, 150 μl) containing blue dye blue, kyoritsu-foods), and a small piece of filter paper (0.5 x 1 cm) placed in the mesh tube was impregnated with odor (1%, 10 μl) or control solution. Flies were allowed to consume sucrose solution for 5 min after which the vials were placed in the freezer (-20 ^{o}C) for at least 1 h. The extent of sucrose consumption by individual flies was quantified under the microscope based on the amount of blue dye in the abdomen, which was scored using the five-point scale ranging from 0 to 2 (Reisenman and Scott, 2019). The scorer was blind to the experimental condition (whether the filter paper in the mesh tube was impregnated with odor or control solvent). For the examination of olfactory organs-removed flies, their third antennal segments and maxillary palps were removed with forceps before starvation.

Electrophysiological recording from taste sensilla on the proboscis

Odor and taste responses of individual taste sensilla on the proboscis were measured using tip recording (Hodgson et al., 1955). Virgin females that had been raised on food for 1-2 days were starved for 24-28 h in vials with water supplied through a wet piece of Kimwipe. Individual flies

bioRxiv preprint doi: https://doi.org/10.1101/2022.03.09.483541; this version posted October 3, 2024. The copyright holder for this preprint (which was not certified by peer review) is the author/funder, who has granted bioRxiv a license to display the preprint in perpetuity. It is made available under aCC-BY-NC-ND 4.0 International license.

were immobilized at the end of a pipette tip. The proboscis was fixed at an extended position using ultraviolet-curing adhesive (NOA 63, Norland). A saline-filled reference electrode was inserted into the eye. Individual taste sensilla were stimulated for ~2 s with a capillary electrode containing the stimulus and an electrolyte, 30 mM TCC. The recording electrode was connected to an amplifier (Multiclamp 700B, Molecular Devices). Signals were bandpass filtered at 100-1000 Hz, and digitally sampled at 10 kHz using a data acquisition module (NI cDAQ9178, NI 9215, National Instruments). The intensity of the response was measured by counting the number of spikes generated between 200 and 700 ms after the stimulus contact following the convention to avoid the contamination of motion artifact (Dahanukar and Benton, 2023) (Delventhal et al., 2014) (Hiroi et al., 2002). Responses to sucrose, banana odor, MCH, and TCC were recorded from L- and I-type sensilla. Sucrose and odors were dissolved in TCC (30 mM) solution. Each stimulus was applied to the same sensillum for 2 or 3 times, with 1 min inter-stimulus-interval. To examine odor-taste integration in each sensillum, banana odor and sucrose solution were presented individually or simultaneously in a mixture. Recordings were made from L2 and L6 sensilla. Each stimulus was presented twice, with 1 min inter-stimulus-interval, in a random order.

Quantification and statistical analysis

Statistical analyses were preformed using Python (3.8.8) or R (4.0.2). A linear model in Figure 3G was generated using Python scikit-learn. Sample sizes are listed in figure legends.

Supplemental information

Figures S1-S9 and Movie S1.

References

Badel, L., Ohta, K., Tsuchimoto, Y., and Kazama, H. (2016). Decoding of Context-Dependent Olfactory Behavior in Drosophila. Neuron *91*, 155-167. 10.1016/j.neuron.2016.05.022.

Boesveldt, S., and de Graaf, K. (2017). The Differential Role of Smell and Taste For Eating Behavior. Perception *46*, 307-319. 10.1177/0301006616685576.

Cameron, P., Hiroi, M., Ngai, J., and Scott, K. (2010). The molecular basis for water taste in Drosophila. Nature *465*, 91-95. 10.1038/nature09011.

Chen, T.W., Wardill, T.J., Sun, Y., Pulver, S.R., Renninger, S.L., Baohan, A., Schreiter, E.R., Kerr, R.A., Orger, M.B., Jayaraman, V., et al. (2013). Ultrasensitive fluorescent proteins for imaging neuronal activity. Nature *499*, 295-300. 10.1038/nature12354.

Dahanukar, A., and Benton, R. (2023). Recording from Fly Taste Sensilla. Cold Spring Harb Protoc

bioRxiv preprint doi: https://doi.org/10.1101/2022.03.09.483541; this version posted October 3, 2024. The copyright holder for this preprint (which was not certified by peer review) is the author/funder, who has granted bioRxiv a license to display the preprint in perpetuity. It is made available under aCC-BY-NC-ND 4.0 International license.

2023, pdb prot108064. 10.1101/pdb.prot108064.

Dahanukar, A., Foster, K., van der Goes van Naters, W.M., and Carlson, J.R. (2001). A Gr receptor is required for response to the sugar trehalose in taste neurons of Drosophila. Nat Neurosci *4*, 1182-1186. 10.1038/nn765.

Dahanukar, A., Lei, Y.T., Kwon, J.Y., and Carlson, J.R. (2007). Two Gr genes underlie sugar reception in Drosophila. Neuron *56*, 503-516. 10.1016/j.neuron.2007.10.024.

Davie, K., Janssens, J., Koldere, D., De Waegeneer, M., Pech, U., Kreft, L., Aibar, S., Makhzami, S., Christiaens, V., Bravo Gonzalez-Blas, C., et al. (2018). A Single-Cell Transcriptome Atlas of the Aging Drosophila Brain. Cell *174*, 982-998 e920. 10.1016/j.cell.2018.05.057.

Delventhal, R., Kiely, A., and Carlson, J.R. (2014). Electrophysiological Recording From Labellar Taste Sensilla. Jove-J Vis Exp. ARTN e51355
10.3791/51355.

Dethier, V.G. (1976). The hungry fly: A physiological study of the behavior associated with feeding.

Devineni, A.V., Sun, B., Zhukovskaya, A., and Axel, R. (2019). Acetic acid activates distinct taste pathways in Drosophila to elicit opposing, state-dependent feeding responses. Elife *8*. 10.7554/eLife.47677.

Dickinson, M.H. (1999). Haltere-mediated equilibrium reflexes of the fruit fly, Drosophila melanogaster. Philos Trans R Soc Lond B Biol Sci *354*, 903-916. 10.1098/rstb.1999.0442.

Dietzl, G., Chen, D., Schnorrer, F., Su, K.C., Barinova, Y., Fellner, M., Gasser, B., Kinsey, K., Oppel, S., Scheiblauer, S., et al. (2007). A genome-wide transgenic RNAi library for conditional gene inactivation in Drosophila. Nature *448*, 151-156. 10.1038/nature05954.

Dweck, H.K.M., and Carlson, J.R. (2023). Diverse mechanisms of taste coding in Drosophila. Sci Adv *9*. ARTN eadj7032
10.1126/sciadv.adj7032.

Endo, K., Tsuchimoto, Y., and Kazama, H. (2020). Synthesis of Conserved Odor Object Representations in a Random, Divergent-Convergent Network. Neuron *108*, 367-381 e365. 10.1016/j.neuron.2020.07.029.

Fujishiro, N., Kijima, H., and Morita, H. (1984). Impulse Frequency and Action-Potential Amplitude in Labellar Chemosensory Neurons of Drosophila-Melanogaster. J Insect Physiol *30*, 317-325. Doi 10.1016/0022-1910(84)90133-1.

Galindo, K., and Smith, D.P. (2001). A large family of divergent Drosophila odorant-binding proteins expressed in gustatory and olfactory sensilla. Genetics *159*, 1059-1072. 10.1093/genetics/159.3.1059.

Haverkamp, A., Yon, F., Keesey, I.W., Mißbach, C., Koenig, C., Hansson, B.S., Baldwin, I.T., Knaden, M., and Kessler, D. (2016). Hawkmoths evaluate scenting flowers with the tip of their proboscis. Elife *5*, e15039.

Hiroi, M., Marion-Poll, F., and Tanimura, T. (2002). Differentiated response to sugars among labellar chemosensilla in. Zool Sci *19*, 1009-1018. DOI 10.2108/zsj.19.1009.

Hodgson, E.S., Lettvin, J.Y., and Roeder, K.D. (1955). Physiology of a Primary Chemoreceptor Unit. Science *122*, 417-418. DOI 10.1126/science.122.3166.417-a.

Inagaki, H.K., Panse, K.M., and Anderson, D.J. (2014). Independent, reciprocal neuromodulatory control of sweet and bitter taste sensitivity during starvation in Drosophila. Neuron *84*, 806-820. 10.1016/j.neuron.2014.09.032.

Jaeger, A.H., Stanley, M., Weiss, Z.F., Musso, P.Y., Chan, R.C., Zhang, H., Feldman-Kiss, D., and Gordon, M.D. (2018). A complex peripheral code for salt taste in Drosophila. Elife *7*. 10.7554/eLife.37167.

Jeong, Y.T., Shim, J., Oh, S.R., Yoon, H.I., Kim, C.H., Moon, S.J., and Montell, C. (2013). An odorant-binding protein required for suppression of sweet taste by bitter chemicals. Neuron *79*,

bioRxiv preprint doi: https://doi.org/10.1101/2022.03.09.483541; this version posted October 3, 2024. The copyright holder for this preprint (which was not certified by peer review) is the author/funder, who has granted bioRxiv a license to display the preprint in perpetuity. It is made available under aCC-BY-NC-ND 4.0 International license.

725-737. 10.1016/j.neuron.2013.06.025.

Jones, W.D., Cayirlioglu, P., Kadow, I.G., and Vosshall, L.B. (2007). Two chemosensory receptors together mediate carbon dioxide detection in Drosophila. Nature *445*, 86-90. 10.1038/nature05466.

Kato, A., Ohta, K., Okanoya, K., and Kazama, H. (2023). Dopaminergic neurons dynamically update sensory values during olfactory maneuver. Cell Rep *42*. ARTN 113122 10.1016/j.celrep.2023.113122.

Kwon, H.W., Lu, T., Rutzler, M., and Zwiebel, L.J. (2006). Olfactory responses in a gustatory organ of the malaria vector mosquito Anopheles gambiae. Proc Natl Acad Sci U S A *103*, 13526-13531. 10.1073/pnas.0601107103.

Kwon, J.Y., Dahanukar, A., Weiss, L.A., and Carlson, J.R. (2007). The molecular basis of CO2 reception in Drosophila. Proc Natl Acad Sci U S A *104*, 3574-3578. 10.1073/pnas.0700079104.

Kwon, J.Y., Dahanukar, A., Weiss, L.A., and Carlson, J.R. (2011). Molecular and cellular organization of the taste system in the Drosophila larva. J Neurosci *31*, 15300-15309. 10.1523/JNEUROSCI.3363-11.2011.

Larsson, M.C., Domingos, A.I., Jones, W.D., Chiappe, M.E., Amrein, H., and Vosshall, L.B. (2004). Or83b encodes a broadly expressed odorant receptor essential for Drosophila olfaction. Neuron *43*, 703-714. 10.1016/j.neuron.2004.08.019.

Larter, N.K., Sun, J.S., and Carlson, J.R. (2016). Organization and function of Drosophila odorant binding proteins. Elife *5*. 10.7554/eLife.20242.

Lee, T., and Luo, L. (1999). Mosaic analysis with a repressible cell marker for studies of gene function in neuronal morphogenesis. Neuron *22*, 451-461. 10.1016/s0896-6273(00)80701-1.

Li, H., Janssens, J., De Waegeneer, M., Kolluru, S.S., Davie, K., Gardeux, V., Saelens, W., David, F., Brbić, M., and Leskovec, J. (2021). Fly Cell Atlas: a single-cell transcriptomic atlas of the adult fruit fly. bioRxiv.

Malik, B., Elkaddi, N., Turkistani, J., Spielman, A.I., and Ozdener, M.H. (2019). Mammalian Taste Cells Express Functional Olfactory Receptors. Chem Senses *44*, 289-301. 10.1093/chemse/bjz019.

Mathis, A., Mamidanna, P., Cury, K.M., Abe, T., Murthy, V.N., Mathis, M.W., and Bethge, M. (2018). DeepLabCut: markerless pose estimation of user-defined body parts with deep learning. Nat Neurosci *21*, 1281-1289. 10.1038/s41593-018-0209-y.

McCrickerd, K., and Forde, C.G. (2016). Sensory influences on food intake control: moving beyond palatability. Obes Rev *17*, 18-29. 10.1111/obr.12340.

Mearns, D.S., Donovan, J.C., Fernandes, A.M., Semmelhack, J.L., and Baier, H. (2020). Deconstructing Hunting Behavior Reveals a Tightly Coupled Stimulus-Response Loop. Curr Biol *30*, 54-69 e59. 10.1016/j.cub.2019.11.022.

Montell, C. (2021). Drosophila sensory receptors-a set of molecular Swiss Army Knives. Genetics *217*, 1-34. 10.1093/genetics/iyaa011.

Ni, L., Bronk, P., Chang, E.C., Lowell, A.M., Flam, J.O., Panzano, V.C., Theobald, D.L., Griffith, L.C., and Garrity, P.A. (2013). A gustatory receptor paralogue controls rapid warmth avoidance in Drosophila. Nature *500*, 580-584. 10.1038/nature12390.

Oh, S.M., Jeong, K., Seo, J.T., and Moon, S.J. (2021). Multisensory interactions regulate feeding behavior in Drosophila. Proc Natl Acad Sci U S A *118*. 10.1073/pnas.2004523118.

Paradis, S., Sweeney, S.T., and Davis, G.W. (2001). Homeostatic control of presynaptic release is triggered by postsynaptic membrane depolarization. Neuron *30*, 737-749. 10.1016/s0896-6273(01)00326-9.

Park, H.-S., and Jun, C.-H. (2009). A simple and fast algorithm for K-medoids clustering. Expert systems with applications *36*, 3336-3341.

bioRxiv preprint doi: https://doi.org/10.1101/2022.03.09.483541; this version posted October 3, 2024. The copyright holder for this preprint (which was not certified by peer review) is the author/funder, who has granted bioRxiv a license to display the preprint in perpetuity. It is made available under aCC-BY-NC-ND 4.0 International license.

Reisenman, C.E., and Scott, K. (2019). Food-derived volatiles enhance consumption in Drosophila melanogaster. J Exp Biol *222*. 10.1242/jeb.202762.

Robertson, H.M., Warr, C.G., and Carlson, J.R. (2003). Molecular evolution of the insect chemoreceptor gene superfamily in Drosophila melanogaster. Proc Natl Acad Sci U S A *100 Suppl 2*, 14537-14542. 10.1073/pnas.2335847100.

Sakoe, H., and Chiba, S. (1978). Dynamic programming algorithm optimization for spoken word recognition. IEEE transactions on acoustics, speech, and signal processing *26*, 43-49.

Schindelin, J., Arganda-Carreras, I., Frise, E., Kaynig, V., Longair, M., Pietzsch, T., Preibisch, S., Rueden, C., Saalfeld, S., Schmid, B., et al. (2012). Fiji: an open-source platform for biological-image analysis. Nat Methods *9*, 676-682. 10.1038/nmeth.2019.

Schwarz, O., Bohra, A.A., Liu, X., Reichert, H., VijayRaghavan, K., and Pielage, J. (2017). Motor control of Drosophila feeding behavior. Elife *6*. 10.7554/eLife.19892.

Scott, K. (2018). Gustatory Processing in Drosophila melanogaster. Annu Rev Entomol *63*, 15-30. 10.1146/annurev-ento-020117-043331.

Scott, K., Brady, R., Jr., Cravchik, A., Morozov, P., Rzhetsky, A., Zuker, C., and Axel, R. (2001). A chemosensory gene family encoding candidate gustatory and olfactory receptors in Drosophila. Cell *104*, 661-673. 10.1016/s0092-8674(01)00263-x.

Shiraiwa, T. (2008). Multimodal chemosensory integration through the maxillary palp in Drosophila. PLoS One *3*, e2191. 10.1371/journal.pone.0002191.

Small, D.M. (2012). Flavor is in the brain. Physiol Behav *107*, 540-552. 10.1016/j.physbeh.2012.04.011.

Spence, C. (2015). Multisensory flavor perception. Cell *161*, 24-35. 10.1016/j.cell.2015.03.007.

Swarup, S., Morozova, T.V., Sridhar, S., Nokes, M., and Anholt, R.R. (2014). Modulation of feeding behavior by odorant-binding proteins in Drosophila melanogaster. Chem Senses *39*, 125-132. 10.1093/chemse/bjt061.

Wang, Z., Singhvi, A., Kong, P., and Scott, K. (2004). Taste representations in the Drosophila brain. Cell *117*, 981-991. 10.1016/j.cell.2004.06.011.

Wieczorek, H., and Wolff, G. (1989). The Labellar Sugar Receptor of Drosophila. J Comp Physiol A *164*, 825-834. Doi 10.1007/Bf00616754.

Wilson, R.I. (2013). Early olfactory processing in Drosophila: mechanisms and principles. Annu Rev Neurosci *36*, 217-241. 10.1146/annurev-neuro-062111-150533.

Xia, Y., and Zwiebel, L.J. (2006). Identification and characterization of an odorant receptor from the West Nile virus mosquito, Culex quinquefasciatus. Insect Biochem Mol Biol *36*, 169-176. 10.1016/j.ibmb.2005.12.003.

Xiang, Y., Yuan, Q., Vogt, N., Looger, L.L., Jan, L.Y., and Jan, Y.N. (2010). Light-avoidance-mediating photoreceptors tile the Drosophila larval body wall. Nature *468*, 921-926. 10.1038/nature09576.

bioRxiv preprint doi: https://doi.org/10.1101/2022.03.09.483541; this version posted October 3, 2024. The copyright holder for this preprint (which was not certified by peer review) is the author/funder, who has granted bioRxiv a license to display the preprint in perpetuity. It is made available under aCC-BY-NC-ND 4.0 International license.

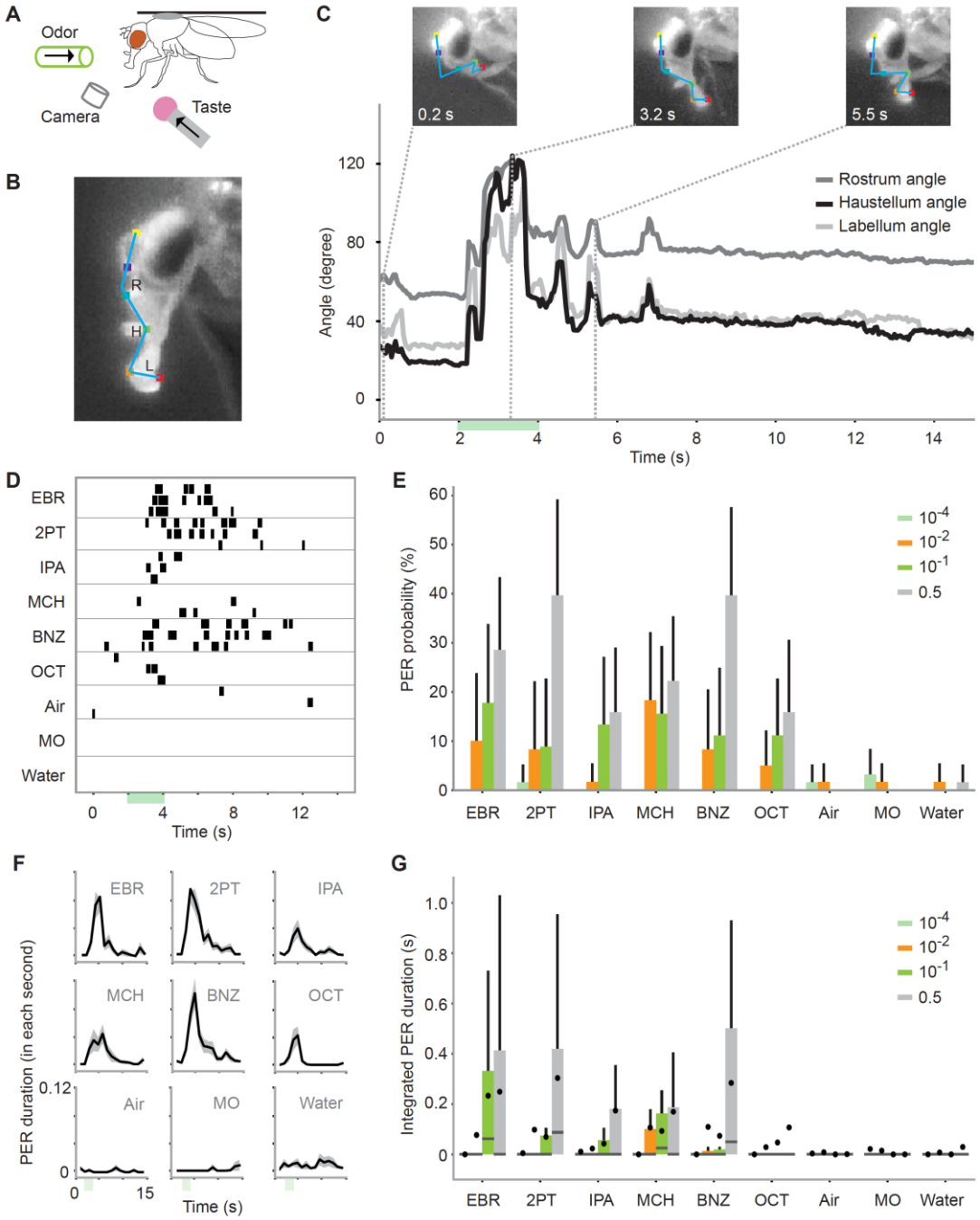

Figure 1. Odors alone evoke PER

(**A**) Schematic for recording odor-evoked PER. (**B**) Six points on the head tracked by DeepLabCut. The movement of the proboscis was characterized by the positions of three segments of the proboscis and the angles between the segments, namely the rostrum angle (R), haustellum angle (H), and labellum angle (L). (**C**) Example odor-evoked PER. Top, images of a proboscis in a retracted (0.2 s), fully extended (3.1 s) and partially extended (5.5 s) state. Bottom,

bioRxiv preprint doi: https://doi.org/10.1101/2022.03.09.483541; this version posted October 3, 2024. The copyright holder for this preprint (which was not certified by peer review) is the author/funder, who has granted bioRxiv a license to display the preprint in perpetuity. It is made available under aCC-BY-NC-ND 4.0 International license.

the three angles over time. Green bar indicates an odor application period. Odor is ethyl butyrate. **(D**) PER to nine odors in an example fly. Each row corresponds to a trial and each tick mark indicates the timing of PER. The odors used are as follows: ethyl butyrate (EBR), 2-pentanone (2PT), isopentyl acetate (IPA), 4-methylcyclohexanol (MCH), benzaldehyde (BNZ), and 3-octanol (OCT). **(E**) PER probability in wild type flies in response to different concentrations of odors. The same stimulus was used for air, mineral oil, and water controls. n = 21, 26, 27, and 28 flies for 10^{-4}, 10^{-2}, 10^{-1}, and 0.5 concentration groups, respectively. Error bar, standard error of the mean. **(F)** PER duration in wild type flies. The black lines indicate the mean and the shaded areas indicate standard error of the mean. n = 28 flies. **(G**) Integrated PER duration in wild type flies in response to different concentrations of odors. The data is from the same flies as in **E**. Box plots indicate the median (gray line), mean (black dot), quartiles (box), and 5-95% range (bar).

bioRxiv preprint doi: https://doi.org/10.1101/2022.03.09.483541; this version posted October 3, 2024. The copyright holder for this preprint (which was not certified by peer review) is the author/funder, who has granted bioRxiv a license to display the preprint in perpetuity. It is made available under aCC-BY-NC-ND 4.0 International license.

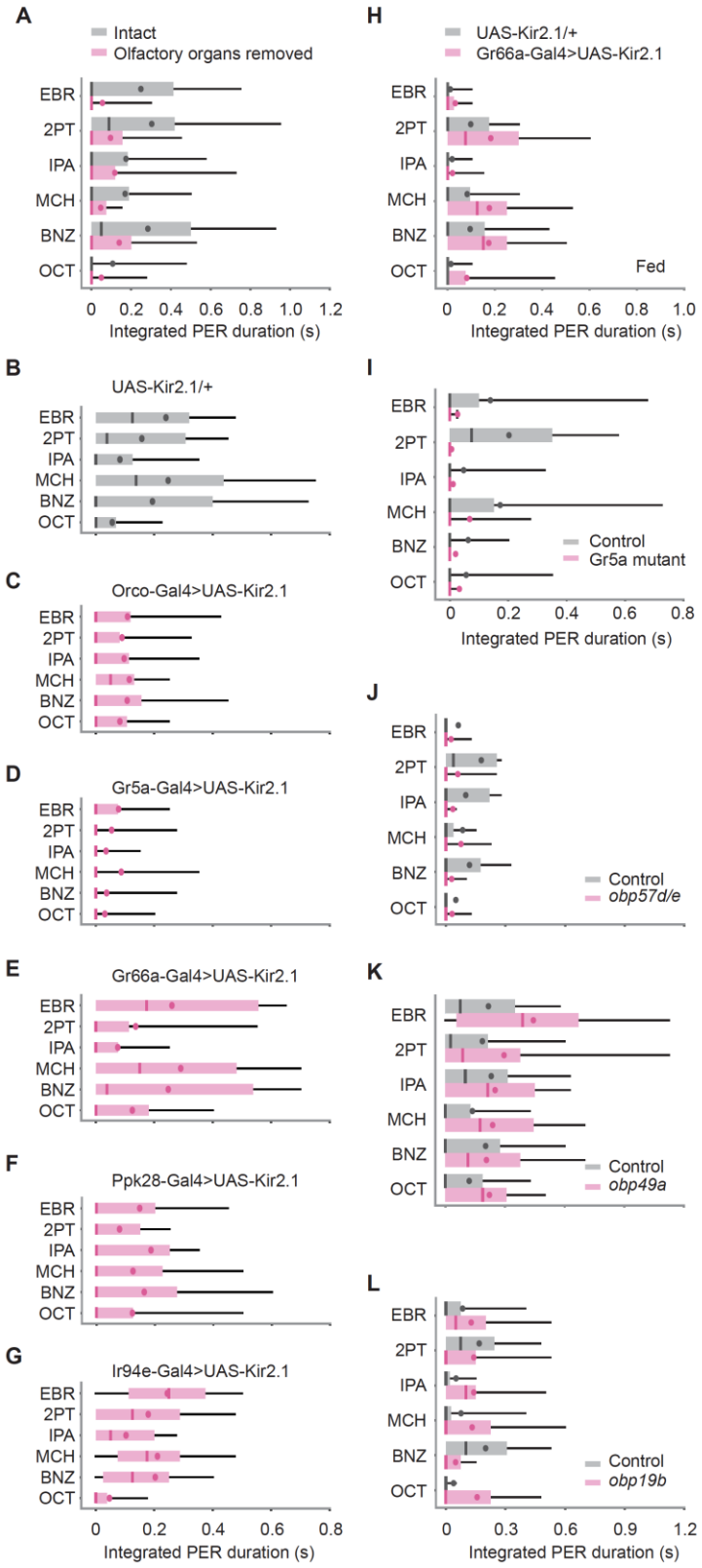

Figure 2. Odors evoke PER through GRNs

bioRxiv preprint doi: https://doi.org/10.1101/2022.03.09.483541; this version posted October 3, 2024. The copyright holder for this preprint (which was not certified by peer review) is the author/funder, who has granted bioRxiv a license to display the preprint in perpetuity. It is made available under aCC-BY-NC-ND 4.0 International license.

(**A**) Integrated PER duration in intact (n = 28) and olfactory organs removed (n = 32) wild type flies. Flies with olfactory organs removed show less PER compared to control flies. p = 0.005. (**B-G**) Integrated PER duration in control (*UAS-Kir2.1*/+, n = 20, **B**), Orco ORN silenced (Orco-Gal4>UAS-Kir2.1, n = 24, **C**), and GRN silenced (Gr5a-Gal4>UAS-Kir2.1, n = 25, **D**; Gr66a-Gal4>UAS-Kir2.1, n = 24, **E**; Ppk28-Gal4>UAS-Kir2.1, n = 28, **F**; Ir94e-Gal4>UAS-Kir2.1, n = 23, **G**) flies. Each silenced line was compared to the control in **B**. p = 0.06, 1e-6, 0.39, 0.10 and 0.12 for **C-G**. Silencing of Orco ORNs and Gr5a GRNs reduce odor-evoked PER. (**H**) Integrated PER duration in control (*UAS-Kir2.1*/+, n = 21) and Gr66a GRN silenced (Gr66a-Gal4>UAS-Kir2.1, n = 21) flies in a fed state. Silencing of Gr66a GRNs enhances odor-evoked PER in a fed state. Odor concentration was 10^{-1}. p = 0.002. (**I**) Integrated PER duration in control (n = 29) and Gr5a mutant (n = 29) flies. PER is severely reduced in mutant flies. p = 1.0e-5. (**J-L**) Integrated PER duration in control and Obp RNAi flies. Obp57d/e RNAi flies show reduced (n = 33 and 25 for control and RNAi), Obp49a RNAi flies show enhanced (n = 24 and 20 for control and RNAi), and Obp19b RNAi flies show similar level of PER (n = 24 and 21 for control and RNAi) as compared to their respective controls. p = 0.006, 0.005, and 0.24 for **J-L**. Scheirer–Ray–Hare test. Box plots indicate the median (gray and red lines), mean (black and red dots), quartiles (box), and 5-95% range (bar).

bioRxiv preprint doi: https://doi.org/10.1101/2022.03.09.483541; this version posted October 3, 2024. The copyright holder for this preprint (which was not certified by peer review) is the author/funder, who has granted bioRxiv a license to display the preprint in perpetuity. It is made available under aCC-BY-NC-ND 4.0 International license.

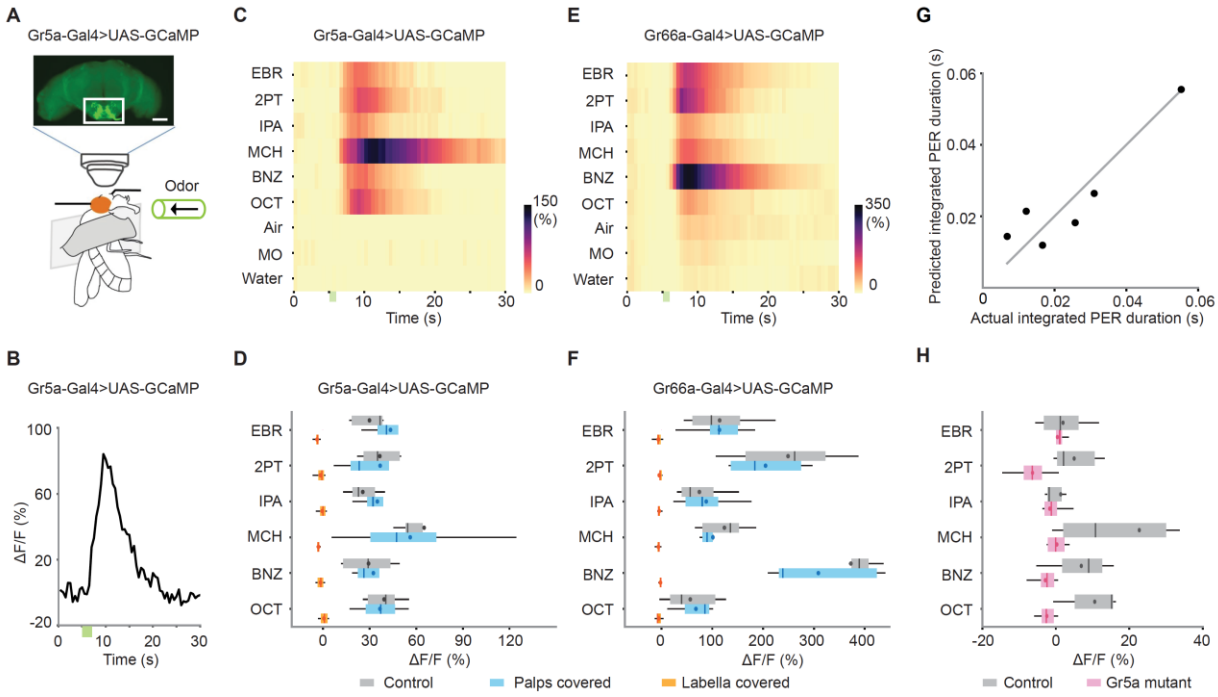

Figure 3. Sweet- and bitter-sensing GRNs directly respond to odors

(**A**) Schematic for two photon calcium imaging of GRN axon termini in the subesophageal zone. The top image shows an anterior view of a brain of Gr5a-Gal4>UAS-GCaMP6s fly. White rectangle indicates the target region of calcium imaging. Scale bar: 50 μm. (**B**) Example response (ΔF/F) to ethyl butyrate. Green bar indicates an odor application period. (**C**) Example responses of Gr5a GRNs to nine odors. Green bar indicates an odor application period. ΔF/F of GCaMP6s fluorescence is color coded according to the scale bar. (**D**) Trial averaged peak responses of Gr5a GRNs to individual odors. Covering the labella (n = 4, p = 2e-13) but not maxillary palps (n = 4, p = 0.15) with glue reduces odor responses as compared to control (n = 5). Two-way ANOVA. (**E**, **F**) Same as in **C**, **D**, but for Gr66a GRNs. As in Gr5a GRNs, covering the labella (n = 5, p = 9e-08) but not maxillary palps (n = 5, p = 0.56) with glue reduces odor responses as compared to control (n = 6). Two-way ANOVA. (**G**) A linear combination of Gr5a and Gr66a GRN responses well predicted the magnitude of odor-evoked PER. PER was measured in Gr5a-Gal4>UAS-GCaMP flies. Each dot represents an odor. Coefficient of determination = 0.81. Weights for Gr5a and Gr66a GRNs are 5e-4 and −2.3e-5, indicating that the former and the latter contributes to enhancement and suppression of PER, respectively. (**H**) Odor responses are severely reduced in Gr5a GRNs in a Gr5a receptor mutant background (n = 6 and 8 for control and mutant, p = 5e-

bioRxiv preprint doi: https://doi.org/10.1101/2022.03.09.483541; this version posted October 3, 2024. The copyright holder for this preprint (which was not certified by peer review) is the author/funder, who has granted bioRxiv a license to display the preprint in perpetuity. It is made available under aCC-BY-NC-ND 4.0 International license.

06, two-way ANOVA). Box plots indicate the median (gray and red lines), mean (black and red dots), quartiles (box), and 5-95% range (bar).

bioRxiv preprint doi: https://doi.org/10.1101/2022.03.09.483541; this version posted October 3, 2024. The copyright holder for this preprint (which was not certified by peer review) is the author/funder, who has granted bioRxiv a license to display the preprint in perpetuity. It is made available under aCC-BY-NC-ND 4.0 International license.

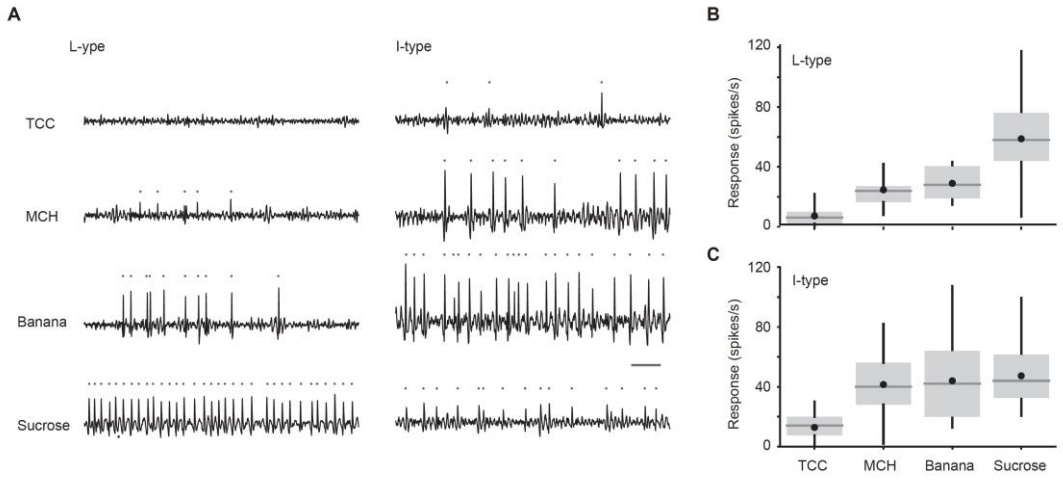

Figure 4. Individual taste sensilla sense odors

(**A**) Example responses of individual taste sensilla recorded using tip recording. Left, example responses to TCC (30 mM), MCH (1%), banana odor (1%), and sucrose (100 mM) recorded in the same L-type sensillum; Right, example responses to the same set of stimuli in the same I-type sensillum. Traces show the activity between 200 and 700 ms after the stimulus onset. Each gray dot indicates a spike. Bar indicates 50 ms. (**B**) Average responses of L-type sensilla. (n = 20, 6, 17, 20 flies for TCC, MCH, banana odor, and sucrose, respectively). Responses to stimuli are significantly larger than those to TCC (p = 3e-18, one-way ANOVA followed by Tukey's HSD, p = 0.02, 0.002, and 2e-7 for MCH, banana, and sucrose compared to TCC in L-type; p = 4e-6, 6e-7, and 1e-8 for MCH, banana, and sucrose compared to TCC in I-type). (**C**) Average responses of I-type sensilla. (n = 30, 9, 22, 30 flies for TCC, MCH, banana odor, and sucrose, respectively). Responses to stimuli are significantly larger than those to TCC (p = 1e-12, one-way ANOVA, post-hoc analysis).

Box plots indicate the median (gray line), mean (black dot), quartiles (box), and 5-95% range (bar).

bioRxiv preprint doi: https://doi.org/10.1101/2022.03.09.483541; this version posted October 3, 2024. The copyright holder for this preprint (which was not certified by peer review) is the author/funder, who has granted bioRxiv a license to display the preprint in perpetuity. It is made available under aCC-BY-NC-ND 4.0 International license.

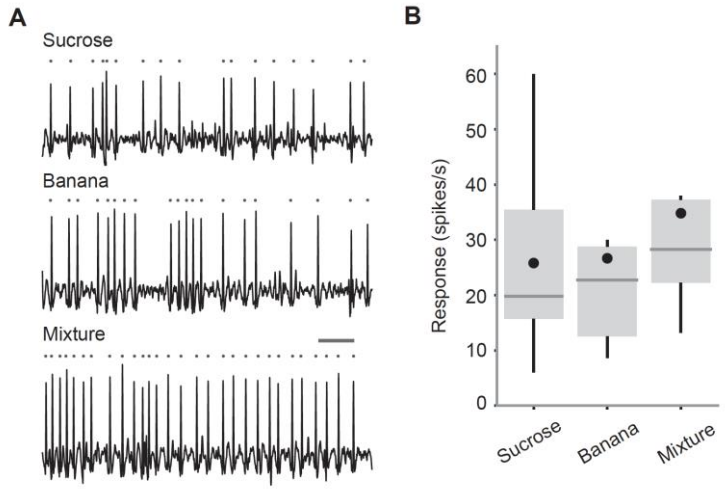

Figure 5. Odor-taste integration in single taste sensillum

(**A**) Example responses of an L-type taste sensillum to sucrose (0.25%, top), banana odor (0.1%, middle) and the mixture of the two (bottom). Traces show the activity between 200 and 700 ms after the stimulus onset. Each gray dot indicates a spike. Bar indicates 50 ms. (**B**) Average responses of L-type sensilla. Responses to the mixture are significantly larger than those to components (n = 14 flies, p = 0.001, repeated measures ANOVA followed by pairwise t-tests with Bonferroni correction, p = 0.003 and 0.003 for sucrose and banana compared to mixture). Box plots indicate the median (gray line), mean (black dot), quartiles (box), and 5-95% range (bar).

bioRxiv preprint doi: https://doi.org/10.1101/2022.03.09.483541; this version posted October 3, 2024. The copyright holder for this preprint (which was not certified by peer review) is the author/funder, who has granted bioRxiv a license to display the preprint in perpetuity. It is made available under aCC-BY-NC-ND 4.0 International license.

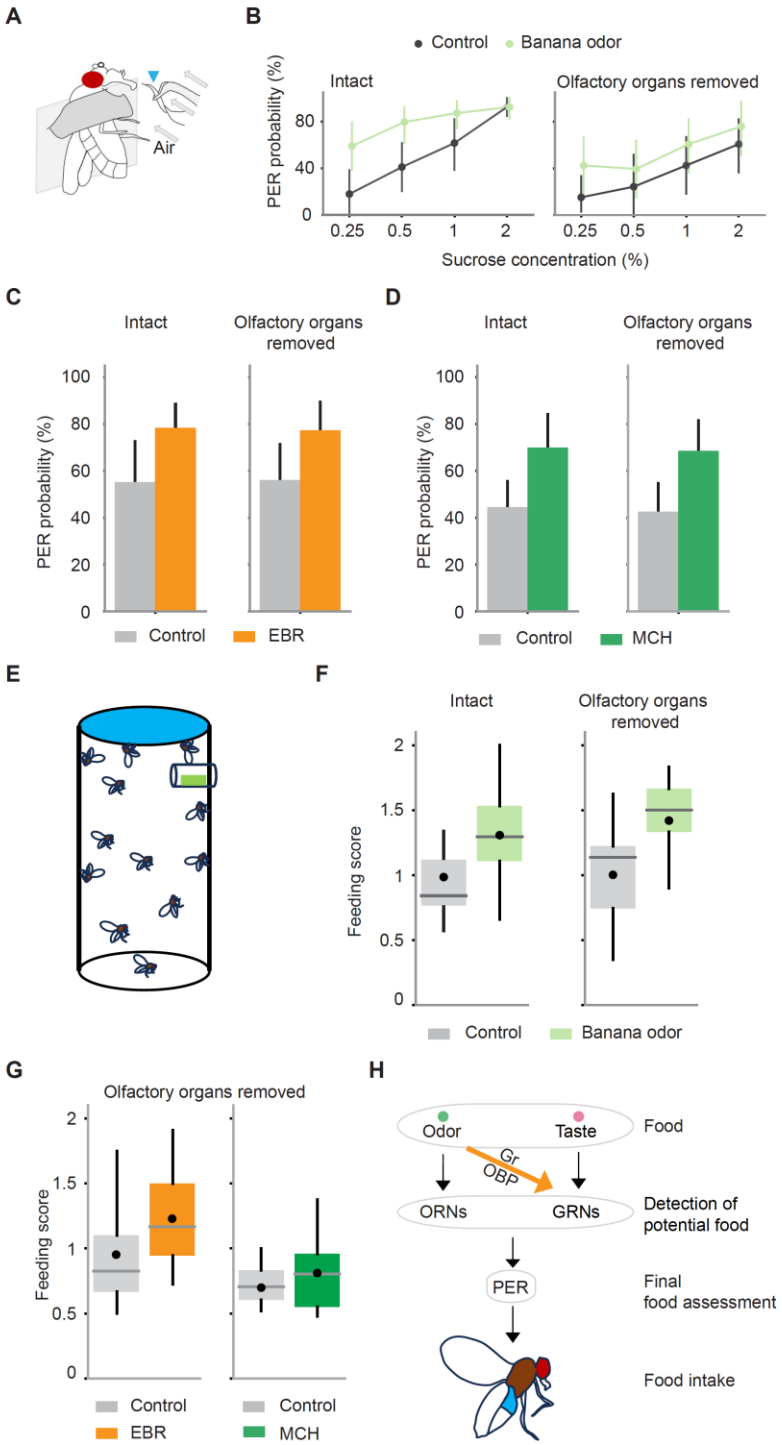

Figure 6. GRNs integrate multisensory input to enhance PER and food consumption

(**A**) Schematic for examining PER in response to odor-taste multimodal stimuli. Stimuli are presented to the labellum with a wick (arrowhead) immersed in a sucrose solution with or without odors. A constant air stream was applied from behind the wick. (**B**) PER probability in response to sucrose at different concentrations with (green) or without (black) banana odor in

bioRxiv preprint doi: https://doi.org/10.1101/2022.03.09.483541; this version posted October 3, 2024. The copyright holder for this preprint (which was not certified by peer review) is the author/funder, who has granted bioRxiv a license to display the preprint in perpetuity. It is made available under aCC-BY-NC-ND 4.0 International license.

wild type flies. Odor concentration was 10^{-4}. Banana odor enhances sucrose-evoked PER even in the absence of olfactory organs (n = 13 and 11, p = 0.002 and 0.04 for intact and olfactory organ-removed flies). Scheirer–Ray–Hare test. Error bar, standard error of the mean. (**C**) PER probability in response to sucrose with or without odors in intact or olfactory organs-removed flies. Odor is EBR (n = 25 and 25, p = 0.005 and 0.007 for intact and olfactory organ-removed flies). Wilcoxon signed-rank test. (**D**) Same as in C, but for MCH (n = 21 and 36, p = 0.007 and 0.0007 for intact and olfactory organs-removed flies). Wilcoxon signed-rank test. The concentration of odors and sucrose was 10^{-4} and 0.25% for C and D. Error bar, standard error of the mean. (**E**) Schematic for quantifying sucrose consumption in the presence or absence of odors. A filter paper on the top was impregnated with sucrose solution containing blue dye and a small piece of filter paper placed in the mesh tube near the top was impregnated with odor or control solution (see STAR Methods). (**F**) The amount of sucrose consumed by flies with or without the presence of banana odor was quantified with a feeding score (see STAR Methods). The amount of feeding was significantly larger in the presence of odor for both intact and olfactory organs-removed flies (n = 13 and 15, p = 0.005 and 0.007 for intact and olfactory organs-removed flies. Wilcoxon signed-rank test. (**G**) The same as in F but with EBR and MCH odors and only for olfactory organs-removed flies (n = 11 and 14, p = 0.03 and 0.24 for EBR and MCH). One-way ANOVA. (**H**) Summary of mechanisms underlying PER and food intake in a multisensory environment.

Error bars are standard error of the mean in bar plots. Box plots indicate the median (gray line), mean (black dot), quartiles (box), and 5-95% range (bar).

bioRxiv preprint doi: https://doi.org/10.1101/2022.03.09.483541; this version posted October 3, 2024. The copyright holder for this preprint (which was not certified by peer review) is the author/funder, who has granted bioRxiv a license to display the preprint in perpetuity. It is made available under aCC-BY-NC-ND 4.0 International license.

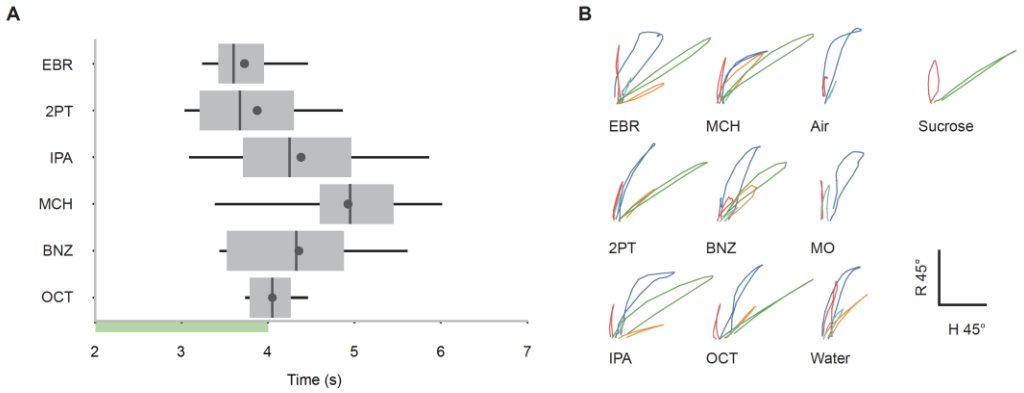

Figure S1. Characteristics of PER in wild type flies, related to Figure 1

(A) Latency to the first odor-evoked PER in wild type flies. Green bar indicates the odor application period. p = 1.0e-4, one-way ANOVA. Box plots indicate the median (gray line), mean (black dot), quartiles (box), and 5-95% range (bar). (**B)** K-medoid clustering of odor- and sucrose-evoked proboscis extensions based on the rostrum and haustellum angles over time in wild type flies. All the trajectories during PER and partial proboscis extensions were clustered into five clusters (color coded), and the representative trajectory closest to each cluster medoid was plotted for each stimulus. The green trajectories represent full extensions that qualify the definition of PER (see Methods). Note that these green trajectories are observed in response to sucrose and all the odors (except for the controls), suggesting that the movement of proboscis during odor-evoked PER is similar to that during sucrose-evoked PER.

bioRxiv preprint doi: https://doi.org/10.1101/2022.03.09.483541; this version posted October 3, 2024. The copyright holder for this preprint (which was not certified by peer review) is the author/funder, who has granted bioRxiv a license to display the preprint in perpetuity. It is made available under aCC-BY-NC-ND 4.0 International license.

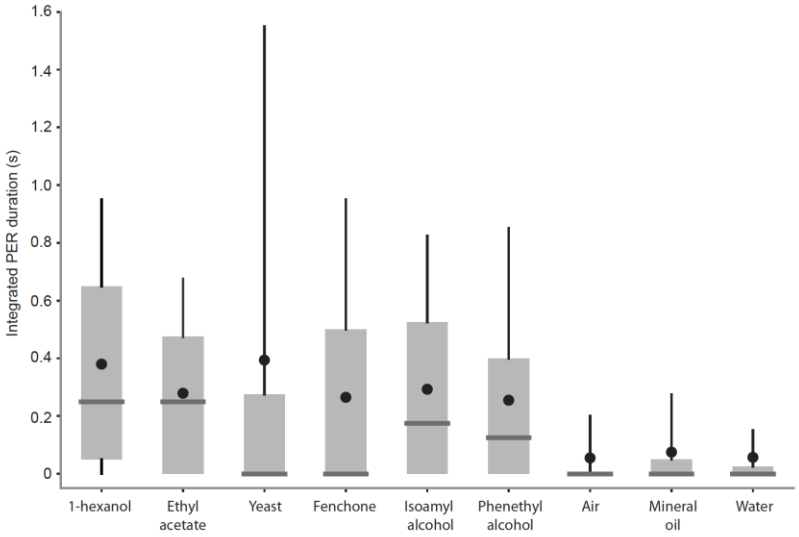

Figure S2. PER evoked by additional odors, related to Figure 1

Integrated PER duration in wild type flies in response to 1-hexanol, ethyl acetate, yeast odor, fenchone, isoamyl alcohol, phenethyl alcohol, air, mineral oil and water. Flies were fixed in a vertical position following a protocol in a previous study (Oh et al., 2021). Box plots indicate the median (gray line), mean (black dot), quartiles (box), and 5-95% range (bar).

bioRxiv preprint doi: https://doi.org/10.1101/2022.03.09.483541; this version posted October 3, 2024. The copyright holder for this preprint (which was not certified by peer review) is the author/funder, who has granted bioRxiv a license to display the preprint in perpetuity. It is made available under aCC-BY-NC-ND 4.0 International license.

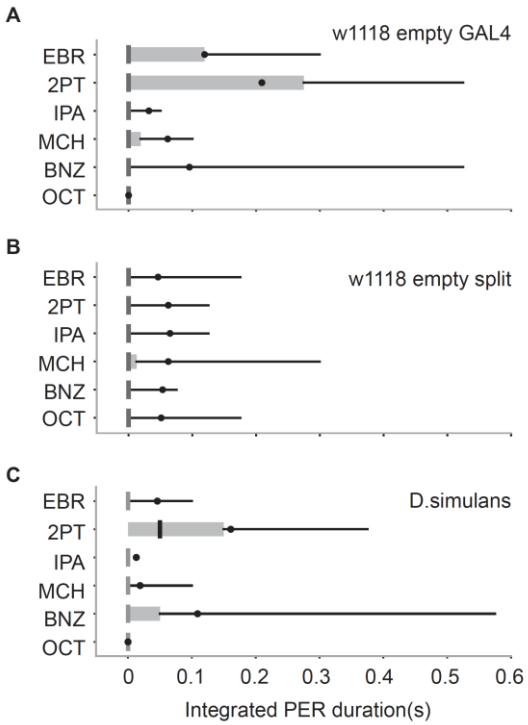

Figure S3. Odor-evoked PER in flies with different genetic backgrounds and in another species, related to Figure1

Integrated PER duration in different flies (n = 20, 28 and 25 in A, B and C). Box plots indicate the median (gray and red lines), mean (black and red dots), quartiles (box), and 5-95% range (bar).

bioRxiv preprint doi: https://doi.org/10.1101/2022.03.09.483541; this version posted October 3, 2024. The copyright holder for this preprint (which was not certified by peer review) is the author/funder, who has granted bioRxiv a license to display the preprint in perpetuity. It is made available under aCC-BY-NC-ND 4.0 International license.

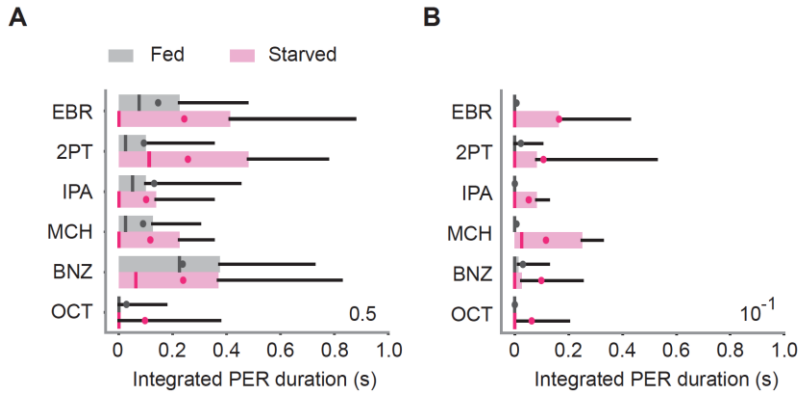

Figure S4. Dependence of odor-evoked PER on a feeding state, related to Figure 2

(**A)** Integrated PER duration in starved (n = 28) and fed (n = 19) wild type flies. PER is enhanced in a starved state (p = 0.88). Scheirer–Ray–Hare test. Odor concentration is 0.5. (**B)** Same as in a but for odor concentration of 10^{-1}. PER is enhanced in a starved state (p = 1e-6). Scheirer–Ray–Hare test. Box plots indicate the median (gray and red lines), mean (black and red dots), quartiles (box), and 5-95% range (bar).

bioRxiv preprint doi: https://doi.org/10.1101/2022.03.09.483541; this version posted October 3, 2024. The copyright holder for this preprint (which was not certified by peer review) is the author/funder, who has granted bioRxiv a license to display the preprint in perpetuity. It is made available under aCC-BY-NC-ND 4.0 International license.

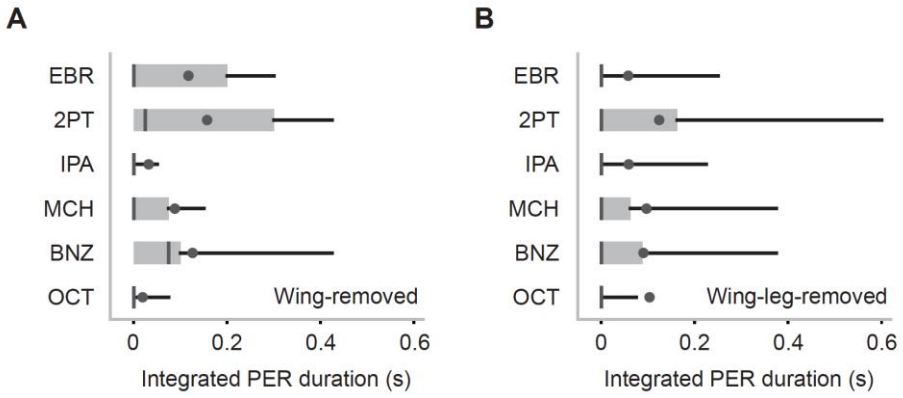

Figure S5. Wings and legs are not required for odor-evoked PER, related to Figure 2

(A) Integrated PER duration in wing-removed Orco-Gal4>UAS-Kir2.1 flies (n = 26). **(B)** Integrated PER duration in wing- and leg-removed, Orco-Gal4>UAS-Kir2.1 flies (n = 27). These results suggest that GRNs in wings and legs are dispensable for odor-evoked PER. Box plots indicate the median (gray line), mean (black dot), quartiles (box), and 5-95% range (bar).

bioRxiv preprint doi: https://doi.org/10.1101/2022.03.09.483541; this version posted October 3, 2024. The copyright holder for this preprint (which was not certified by peer review) is the author/funder, who has granted bioRxiv a license to display the preprint in perpetuity. It is made available under aCC-BY-NC-ND 4.0 International license.

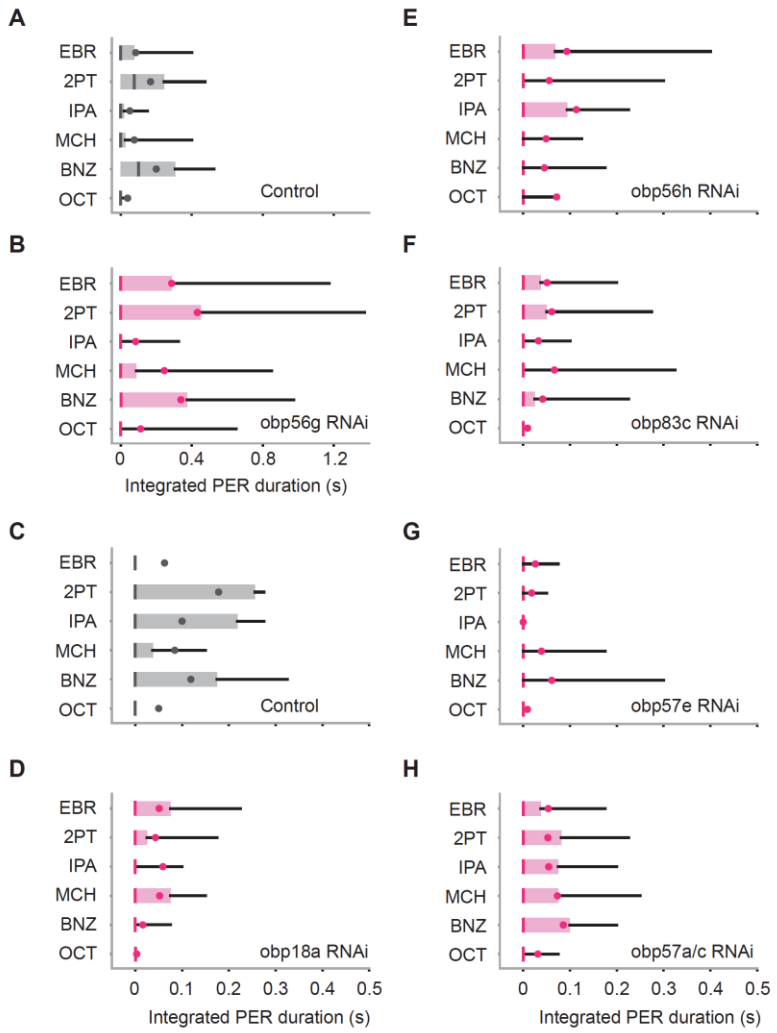

Figure S6. Contributions of OBPs to odor-evoked PER, related to Figure 2

(A, B) Integrated PER duration in control and Obp56g RNAi flies. These flies show similar level of PER (n = 24 and 23 for control and RNAi, p = 0.58). Scheirer–Ray–Hare test. (**C-H)** Integrated PER duration in control and OBP RNAi flies. Obp18a RNAi and Obp57e RNAi flies show reduced level of PER as compared to control (n = 33, 25, 22, 25, 27, and 28 flies for **C-H**, p = 0.05, 0.36, 0.08, 0.05, and 0.90 for **D-H**). Scheirer–Ray–Hare test. Box plots indicate the median (gray and red lines), mean (black and red dots), quartiles (box), and 5-95% range (bar).

bioRxiv preprint doi: https://doi.org/10.1101/2022.03.09.483541; this version posted October 3, 2024. The copyright holder for this preprint (which was not certified by peer review) is the author/funder, who has granted bioRxiv a license to display the preprint in perpetuity. It is made available under aCC-BY-NC-ND 4.0 International license.

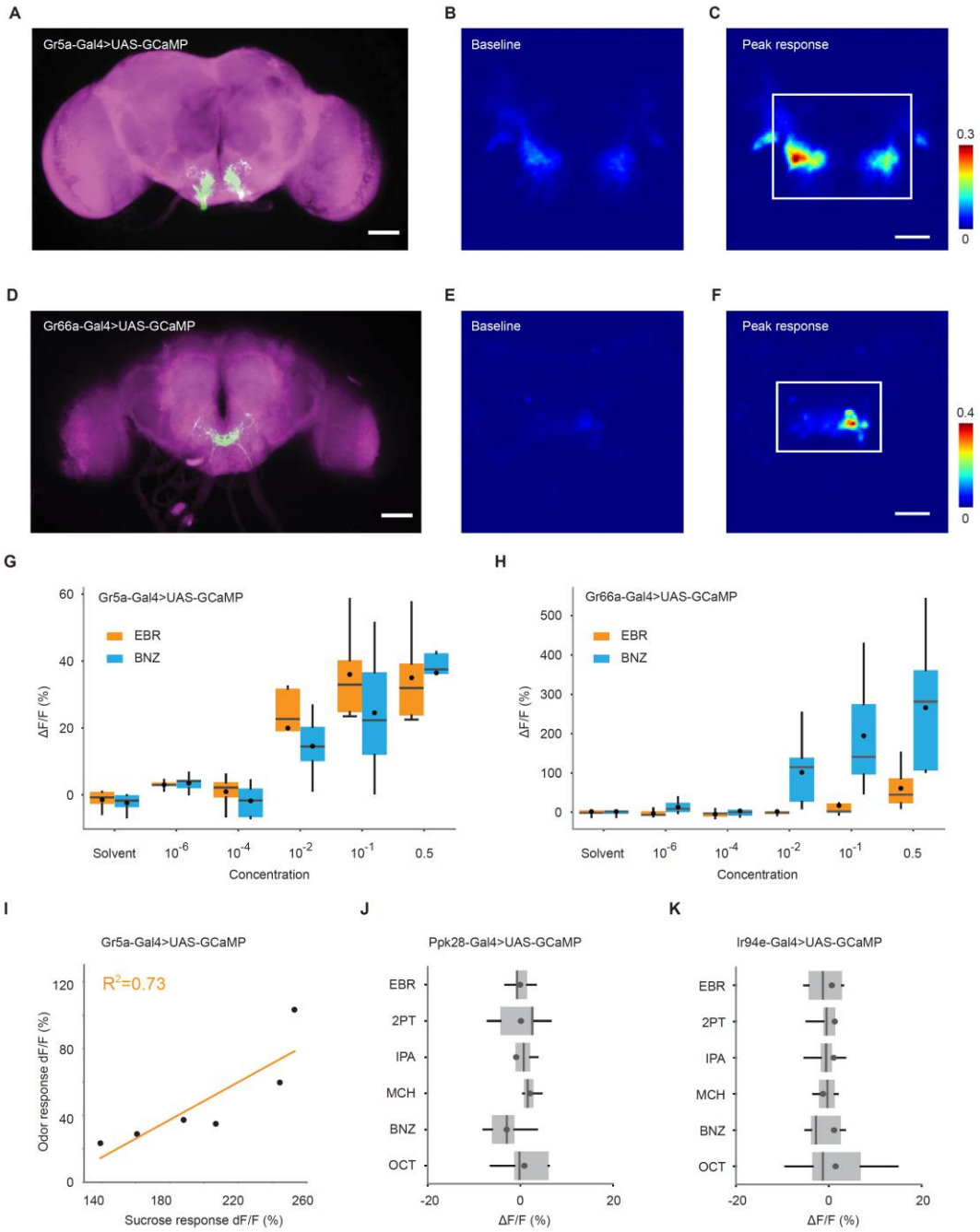

Figure S7. Responses of GRNs to odors and sucrose, related to Figure 3

(A) Image of a brain of Gr5a-Gal4>UAS-GCaMP6s fly, stained with anti-GFP to reveal Gr5a neurons (green) and nc82 to reveal synapses (magenta). Scale bar, 50 µm. (**B)** Baseline florescence intensity of GCaMP6s in Gr5a GRNs. Fluorescence (arbitrary unit) is color coded according to the scale bar. **(C)** Peak florescence intensity of GCaMP6s in the same fly as shown in B after stimulation with 4-methylcyclohexanol. Fluorescence is color coded according to the

bioRxiv preprint doi: https://doi.org/10.1101/2022.03.09.483541; this version posted October 3, 2024. The copyright holder for this preprint (which was not certified by peer review) is the author/funder, who has granted bioRxiv a license to display the preprint in perpetuity. It is made available under aCC-BY-NC-ND 4.0 International license.

scale bar. The ROI used for ΔF/F calculation is indicated by a white rectangle. Scale bar, 20 μm. (**D-F)** Same as in **A-C**, but for Gr66a-Gal4>UAS-GCaMP6s fly and benzaldehyde stimulation. (**G)** Trial averaged peak responses of Gr5a GRNs to different concentrations of ethyl butyrate (EBR) and benzaldehyde (BNZ). n = 5 flies. (**H)** Same as in **G,** but for Gr66a GRNs. **(I)** Responses to 4-methylcyclohexanol is positively correlated with that to sucrose (0.25%) in Gr5a GRNs. Each dot corresponds to a fly. (**J)** Trial averaged peak responses of Ppk28 GRNs to individual odors. These neurons do not respond to odors. n = 5 flies. (**K)** Same as in **J**, but for Ir94e GRNs. n = 9 flies. Box plots indicate the median (gray line), mean (black dot), quartiles (box), and 5-95% range (bar).

bioRxiv preprint doi: https://doi.org/10.1101/2022.03.09.483541; this version posted October 3, 2024. The copyright holder for this preprint (which was not certified by peer review) is the author/funder, who has granted bioRxiv a license to display the preprint in perpetuity. It is made available under aCC-BY-NC-ND 4.0 International license.

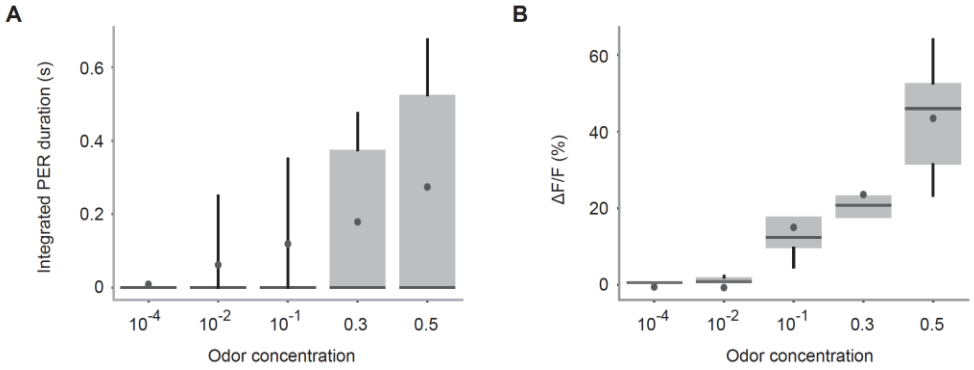

Figure S8. PER and GRN responses to various concentrations of banana odor, related to Figure 3

(A) Integrated PER duration in response to a banana odor presented at various concentrations in wild type flies. n = 21 flies. Box plots indicate the median (gray line), mean (black dot), quartiles (box), and 5-95% range (bar). (**B)** Trial averaged peak responses of Gr5a GRNs in response to various concentrations of banana odor in Gr5a-Gal4>UAS-GCaMP6s flies. n = 5 flies. Error bar, standard error of the mean.

bioRxiv preprint doi: https://doi.org/10.1101/2022.03.09.483541; this version posted October 3, 2024. The copyright holder for this preprint (which was not certified by peer review) is the author/funder, who has granted bioRxiv a license to display the preprint in perpetuity. It is made available under aCC-BY-NC-ND 4.0 International license.

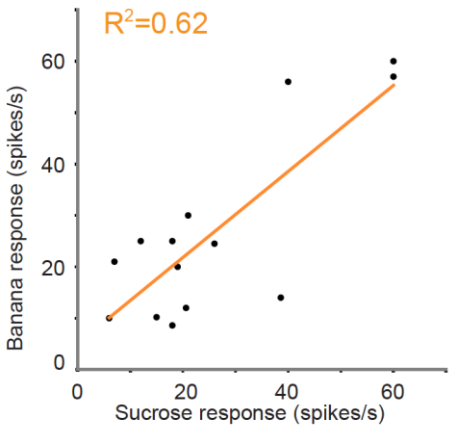

Figure S9. Correlation between odor and taste responses in individual sensilla, related to Figure 5

Spike responses to banana odor (0.01%) are positively correlated with those to sucrose (0.25%) in L-type sensilla. Each dot corresponds to a fly.

Movie S1. Odor-evoked PER, related to Figure 1

A movie capturing odor-evoked PER with the plot of haustellum angle over time. Six points on the head were tracked by DeepLabCut.